Studies on foam in porous media and the effect of oil

Hussain, Ahmed

DOI
10.4233/uuid:ad56c73d-4986-4358-9dd2-2929004cea6f

Publication date
2019

Document Version
Final published version

Citation (APA)
Hussain, A. (2019). *Studies on foam in porous media and the effect of oil*. [Dissertation (TU Delft), Delft University of Technology]. https://doi.org/10.4233/uuid:ad56c73d-4986-4358-9dd2-2929004cea6f

STUDIES ON FOAM IN POROUS MEDIA AND THE EFFECT OF OIL

AHMED AMIR ABDULKEREEM HUSSAIN

STUDIES ON FOAM IN POROUS MEDIA AND THE EFFECT OF OIL

PROEFSCHRIFT

ter verkrijging van de graad van doctor
aan de Technische Universiteit Delft,
op gezag van de Rector Magnificus prof.dr.ir. T.H.J.J. van der Hagen
voorzitter van het College voor Promoties,
in het openbaar te verdedigen op
woensdag, 26 juni, 2019 om 15:00 uur

door

Ahmed Amir Abdulkereem HUSSAIN
Master of Science in Applied Earth Sciences,
Technische Universiteit Delft, Nederland
geboren te Zaanstad, Nederland

Dit proefschrift is goedgekeurd door de promotor

Samenstelling promotiecommissie bestaat uit:

Rector magnificus,	voorzitter
Prof. dr. W. R. Rossen	Technische Universiteit Delft, promotor

Onafhankelijke leden:

Prof. dr. H. Bertin	Université de Bordeaux
Prof. dr. ir. R. A. W. M. Henkes	Technische Universiteit Delft
Prof. dr. P. L. J. Zitha	Technische Universiteit Delft
Dr. J. Gebert	Technische Universiteit Delft
Dr. I. M. Saaid	Universiti Teknologi PETRONAS

Overig lid:

Dr. S. Y. F. Vincent-Bonnieu	Shell Global Solutions International BV/ Technische Universiteit Delft

Dr. S. Y. F. Vincent-Bonnieu heeft als begeleider in belangrijke mate aan de totstandkoming van het proefschrift bijgedragen.

This doctoral research was sponsored by Universiti Teknologi PETRONAS.

ISBN 978-94-6366-190-4

Table of contents

1. Introduction

1.1. Rationale

For conventional oil fields, typically only 35% of the oil initially in the reservoir is produced by the time the operator abandons the field. Thus, it is not uncommon for a company that discovers an oil field containing 100 million barrels of oil, to develop and exploit it, and finally abandon the field with 65 million barrels left in the ground. Usually companies abandon the field because they are not technically capable to produce more oil economically (Lake et al., 2014). In this chapter we give an introduction to conventional methods to produce oil from a reservoir and on applying foam to enhance oil recovery (EOR).

In order to unlock the oil that is trapped in the pores of the rock of the reservoir, the operator usually drills injection wells and production wells into the reservoir. This allows the operator to inject water and/or gas into the reservoir to displace oil towards the production wells. A benefit of injecting gas is that it displaces more oil from the pores it sweeps than water; gas flooding results in a higher *microscopic sweep efficiency* than water flooding. However, compared to water, it flows through the upper layer of the reservoir due to gravity override; water flooding can result in a higher *volumetric sweep efficiency* than gas flooding. This is because of three reasons: density difference between gas and crude oil, viscosity difference between gas and crude oil and gas prefers to flow through higher-permeability layers in a reservoir. Firstly, because gas is less dense than crude oil it has the tendency to *override* the oil in the reservoir, and move along the upper part of the reservoir. Similarly, because water is usually denser than crude oil, injected water will likely *underride* oil and move along the lower part of the reservoir. Secondly, because gas is less viscous than crude oil, it is more likely to *finger* through the crude oil than water. Thirdly, if an operator gas-floods a reservoir which has a thin streak of sand with relatively large pores, the gas will tend to flow through the thin streak of sand, bypassing the rest of the reservoir.

Foam is gas dispersed, i.e. as bubbles, in a continuous liquid phase (Haynes, 2016). Foam effectively traps gas in the pores. It can improve the volumetric sweep efficiency of a gas displacement by reducing the gas mobility. In practical terms, foam behaves as a high-viscosity gas in the reservoir, with a higher viscosity in layers with higher permeability (Kapetas et al., 2015b; Raza, 1970). These foam characteristics make it a viable option for improving gas-flooding.

In this work, we model surfactant depletion by the gas-water interface, which can be used to gain information on the surfactant concentration necessary to stabilize foam in a porous medium. Furthermore, we focus on how the foam behaves in presence of the crude oil in a porous medium.

1.2. Foam stability

1.2.1. Foam stability in absence of oil

Foam stays stable for a finite period of time (Haynes, 2016). The three (interlinked) mechanisms that contribute to the destabilization and finally destruction of foam are coarsening, liquid drainage and collapse. Coarsening is the diffusion of gas from one gas bubble to another bubble. Liquid drainage is the following phenomenon: liquid that is situated between the foam films (called lamellae) and in the Plateau borders will flow downward due to gravity and due to capillary suction in the Plateau borders. In a porous medium, if the surrounding capillary pressure

is greater than that in the foam, liquid drains out to nearby pores. Over time, as foam loses liquid, capillary pressure rises. The lamellae between bubbles break when capillary pressure reaches a critical value, which depends on surfactant, salinity, temperature, and other factors. Collapse is the phenomenon of the lamella between two bubbles breaking, merging the bubbles to form a single foam bubble.

Figure 1.1 shows three gas bubbles, with lamellae between them, and a Plateau border (called P_{pb} in the figure). The pressure in the lamella is different from that in the Plateau border because the two surfaces of the foam lamellae repel each other due to electrostatic and other forces between the surfaces. The proximity of ions with similar charges and steric effects cause repulsive forces. Attractive van der Waals forces play a role as well (Farajzadeh et al., 2012). The repulsive force per unit area is represented as a pressure to be included in the equilibrium condition and is known as the disjoining pressure (Π) (Bergeron, 1997), which can be divided into the , which can be divided into the electrostatic Π_{EL}, steric Π_{ST}, and van der Waals Π_{VW} forces. The pressure difference across the gas-liquid interface is the capillary pressure; see Eq. 1.1. In equilibrium the capillary pressure is equal to the disjoining pressure in a lamella; see Eq. 1.2.

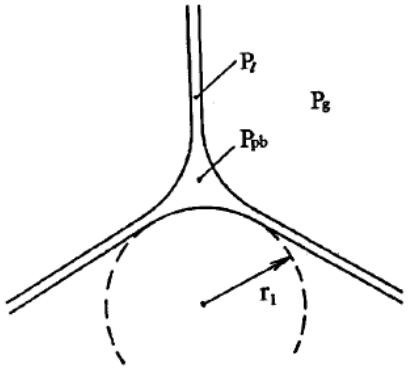

Figure 1.1: Illustration of three similar gas bubbles, with lamellae between pair of bubbles (pressure = P_l), and a Plateau border (pressure = P_{pb} = P_{liq}); from Kornev et al. (1999).

$$P_c = P_{gas} - P_{liq} \qquad \textbf{Eq. 1.1}$$

$$\Pi(\mathrm{h}) = \Pi_{\mathrm{EL}} + \Pi_{\mathrm{ST}} + \Pi_{\mathrm{VW}} = P_c, in\ equilibrium \qquad \textbf{Eq. 1.2}$$

The van der Waals component of the disjoining pressure has a negative sign in symmetric foam lamellae. In asymmetric lamellae the contribution of Π_{VW} can be positive and therefore this force can be attractive or repulsive. If $\Pi_{EL} > \Pi_{VW} + P_C$ the lamella surfaces are well separated, and thus the foam lamella and the foam are stable. If the negative component of Π is stronger (i.e. $\Pi_{EL} < \Pi_{VW} + P_C$), the two foam lamella surfaces come into contact, the lamella collapses and the foam is unstable (Farajzadeh et al., 2012).

The disjoining pressure can be determined experimentally. The measured disjoining pressure curve can be described with the Derjaguin-Landau-Verwey-Overbeek (DLVO) theory. The DLVO theory combines electrostatic forces, which tend to stabilize the lamellae, and van der Waals forces, which tend to destabilize the foam lamella. Figure 1.2 gives an illustration of typical disjoining pressure isotherms. Π_c is the critical disjoining pressure, at which rupture takes place in a static lamella. Since at equilibrium the disjoining pressure equals the capillary pressure, this is

also the value of the critical capillary pressure. Similarly, in porous media, foam coarsens at the limiting capillary pressure (P_c^*), which is somewhat greater than the critical value measured for static lamellae. P_c^* for foam in porous media increases with surfactant concentration, even above the critical micelle concentration (CMC) (Khatib et al., 1988); the critical capillary pressure for static lamellae does not increase above the CMC. As one reduces water fractional flow in a foam there is a transition in behaviour as foam reaches its limit of stability. This transition fractional flow is denoted as f_w^*.

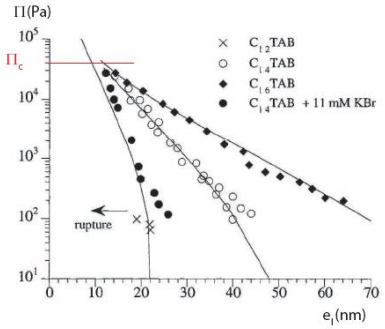

Figure 1.2: This figure shows an example of disjoining pressure vs. lamella thickness. These were measured with C_nTAB surfactant solutions. Π_c denotes the critical disjoining pressure. Adapted from Bergeron (1997).

1.2.2. Foam stability in the presence of oil

Crude oil can significantly change the behaviour foam in a porous medium (Raza, 1970; Schramm et al., 1993). When designing a foam-flood for EOR purposes, the ideal foam behaviour in the presence of oil depends on the foam utilization objective. The objective can be to have the foam displace the oil, whereby the foam acts as a possible alternative to polymer-thickened water (Lawson and Reisberg, 1980). In this case, it is not ideal if the foam completely collapses in contact with oil. Foam can also be injected with the objective to have it divert flow of the following injectant to an oil-rich layer. In this case foam reduces mobility in oil-poor layers, so that when the operator switches from injecting foam to another fluid (such as CO_2, other gases or acid) the foam diverts the injected fluid (Holm and Garrison, 1988; Rossen et al., 2016). For such an application it might be preferred to have stable foam in the oil-poor layer and to have foam collapse in the oil-rich layer.

Because the behaviour of foam in the presence of crude oil is an important factor in a successful application of foam for EOR purposes, the behaviour of foam in the presence of crude oil is usually experimentally investigated before application. The experimental results allow the operator to model the behaviour of foam in the presence of crude oil and predict the incremental oil to be recovered by foam application. Bulk foams, i.e. foam in a column, test tube or other container much larger than the bubbles, are sometimes used as a cost-effective surfactant-screening tool for EOR (Andrianov et al., 2012; Boeije et al., 2017; Suffridge, 1989; Turta and Singhal, 2002). However, the behaviour of foam and oil in bulk is not necessarily correlated to the behaviour of foam and oil flowing in a porous medium. Therefore it is necessary to conduct core-flood experiments to understand the flow behaviour of foam in porous media (Andrianov et al., 2012; Jones et al., 2016b; Suffridge, 1989). In the next section we discuss a thermodynamic method to predict the behaviour of foam in the presence of oil, using only the interfacial tensions between the three phases (surfactant solution, gas and oil).

1.2.2.1. Foam in contact with oil: stability theory based on thermodynamics: the entering/spreading/bridging coefficients

The "Bridging-Spreading" mechanism is commonly used to predict foam stability in the presence of oil whether an oil droplet entering the gas-water interface lowers total interfacial energy; see Eq. 1.3:

$$E_{o/w} = \sigma_{wg} + \sigma_{ow} - \sigma_{og} \qquad \textbf{Eq. 1.3}$$

where σ_{wg}, σ_{ow} and σ_{og} are the interfacial tensions between water and gas, oil and water, and oil and gas respectively. If $E_{o/w} < 0$, the oil droplet remains within the aqueous phase (i.e., not break through to the gas-water interface) and thus the foam will be stable. It is thermodynamically favourable for the oil droplet to enter the gas-water interface if $E_{o/w} > 0$.

The spreading coefficient, $S_{o/w}$, gives information on the thermodynamic favourability of spreading of an oil droplet over the gas-water interface; see Eq. 1.4. Specifically, it identifies whether interfacial energy is reduced if the oil forms a thin layer on top of the lamella. If the entering coefficient and spreading coefficient are both positive, it is favourable for the oil droplet to enter and then spread over the gas-water interface, resulting in the gas-water interface to expand and the lamella to thin; it can rupture because of that.

$$S_{o/w} = \sigma_{wg} - (\sigma_{ow} + \sigma_{og}) \qquad \textbf{Eq. 1.4}$$

The bridging coefficient (B) gives an indication whether the water will move away from the oil drop for the cases that oil enters the gas-water interface, but does not spread over the gas-water interface; see Eq. 1.5. If the bridging coefficient is positive, a capillary pressure will occur in the lamella that will force the water to move away from the oil drop. The oil drop enters both surfaces of the lamella, i.e. the droplet forms an unstable bridge across the lamella. For negative values of the bridging coefficient, the spreading coefficient is negative as well (see Eq. 1.4); thus spreading and bridging will not take place.

$$B = \sigma_{wg}^2 + \sigma_{ow}^2 - \sigma_{og}^2 \qquad \textbf{Eq. 1.5}$$

1.2.2.2. Lamella coefficient for predicting foam breakage by oil droplets

The lamella theory is a proposed mechanism for predicting foam stability that incorporates oil emulsification and imbibition in the foam structure (Schramm et al., 1993; Schramm and Novosad, 1992). If small oil droplets are formed by emulsification, they will be able to move to the inside of the foam structure.

The capillary suction in the Plateau border draws oil into the Plateau border, where a pinch-off mechanism produces emulsified oil; see Eq. 1.6, where r_p is equal to the radius of the Plateau border:

$$\Delta p_c = \frac{2\sigma_{wg}}{r_p} \qquad \textbf{Eq. 1.6}$$

The pressure difference across an oil-water interface can be calculated with Eq. 1.7, where r_o is the radius of curvature of the oil surface:

$$\Delta p_R = \frac{2\sigma_{ow}}{r_o} \qquad \textbf{Eq. 1.7}$$

The *Lamella number* (Eq. 1.8) is a dimensionless number that gives an indication of the foam stability. It is the ratio of Δp_c over Δp_R. The foam will be stable for a lamella number smaller than one, semi-stable for values between one and seven, and unstable for values larger than seven according to Schramm et al. (1993); see Figure 1.3. Schramm and Novosad (1992) found that r_o/r_p was equal to 0.15 in their microfluidic experiments, where it was possible to see the size of the oil droplets and Plateau borders.

$$L = \frac{\Delta p_c}{\Delta p_R} = \frac{r_o}{r_p}\frac{\sigma_{wg}}{\sigma_{ow}} \qquad \textbf{Eq. 1.8}$$

Van der Bent (2014) investigated the reliability of the E/S/B coefficients and the lamella number predictions for foam behaviour in the presence of oil in bulk, in microfluidics and in porous media. He finds these models are unreliable for foam in porous media, and ambiguous for foam in microfluidics and in bulk Table 1.1.

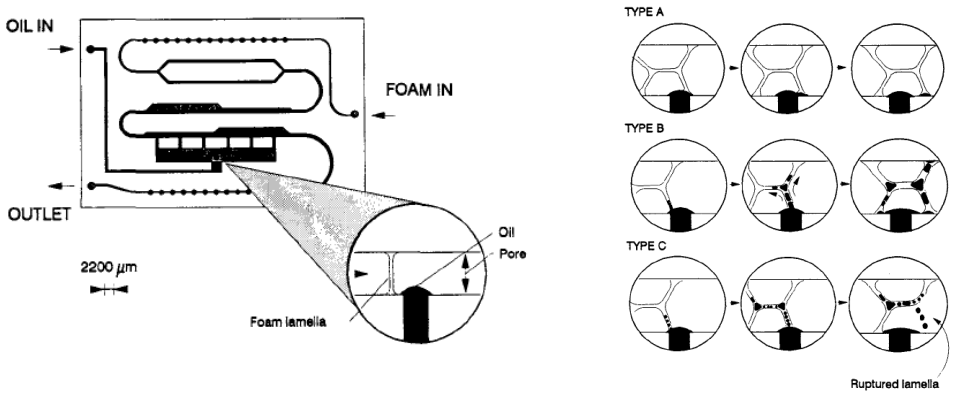

Figure 1.3: The image on the left is the microfluidic cell plate used for the experiments leading to the lamella theory for foam stability in contact with oil. The image on the right is an illustration of the different types of foam behaviour in contact with oil, courtesy of Schramm et al. (1993).

Table 1.1: A summary of foam-stability predictions based on the entering, spreading and bridging coefficients and the lamellae number compared with the experimental findings of different authors. If the results of the authors are in agreement with the stability criteria the reference is given in black; otherwise the reference is given in red. Adapted from Van der Bent (2014).

Stability criteria	Predicted foam stability	Bulk foam	Micro model	Porous media
$E < 0$	Stable		Denkov et al. (2014)	Mannhardt et al. (2000) Bergeron et al. (1993) Dalland et al. (1994)
$E > 0$, $B < 0$	Stable	Denkov et al. (2014)		
$E > 0$, $B > 0$, $S > 0$	Unstable	Simjoo et al. (2013) Denkov et al. (2014) Lau and O'Brien (1988)	Manlowe and Radke (1990) Koczo et al. (1992)	Kristiansen and Holt (1992) Dalland et al. (1994) Lee et al. (2013)
$E > 0$, $B > 0$, $S < 0$	Unstable	Denkov et al. (2014)		Mannhardt et al. (2000) Dalland et al. (1994)
$L < 0$	Stable		Schramm and Novosad (1992)	Andrianov et al. (2012)
$1 > L < 5.5$	Intermediate	Vikingstad et al. (2005)		Bergeron et al. (1993)
$L > 5.5$	Unstable			Dalland et al. (1994)

Foam stability theory, described above with thermodynamic coefficients, determine if it is energetically favourable for an oil droplet to have a particular configuration. However, oil and foam are under dynamic conditions in a porous medium. This might be one of the reasons why thermodynamic properties of the surfactant/oil mixture cannot fully predict the behaviour of the oil drops with foam (Schramm and Novosad, 1992).

1.2.3. Foam generation in EOR applications

Two methods to generate foam in porous media are co-injection of gas and surfactant and alternating injection of surfactant and gas slugs (SAG) (Farajzadeh et al., 2012; Jensen and Friedmann, 1987). Bond and Holbrook (1958) were the first to propose the use of foam for gas mobility control, after which several successful field applications of foam (in a pilot scale) have followed. Some examples are the East Vacuum field in the USA, and the Oseberg field and the Snorre field offshore Norway (Lee and Kam, 2013; Martin et al., 1995; Patzek, 1996; Skauge et al., 2002; Turta and Singhal, 2002).

1.3. Research questions, hypotheses and objectives

This work is aimed at providing insights into the following research topics:

- Our first question: why does the transition water fractional flow, f_w^*, of foam in porous media decrease with increasing surfactant concentration, well above the CMC?
    - Our hypothesis is that a higher surfactant concentration than the CMC is needed to saturate the gas-water interfaces of foam in porous media.

  - Our first objective is to quantify surfactant depletion by the gas-water interfaces of a foam at the transition water fractional flow, f_w^*. This is relevant because the surfactant molecules adsorbed to the gas-water interfaces stabilize foam. A better understanding of surfactant depletion by the gas-water interfaces can be used by an operator to tailor the surfactant concentration to optimize process objectives.
- Our second question: what characteristic of a crude-oil determines its impact on a foam?
  - Our hypothesis is that the impact of a crude-oil on foam is the summation of the impact of the different crude oil components.
  - Our second objective is to describe the impact of one specific crude oil on foam based on the impact of some of the crude oil components. This can be seen as a starting step in a method to predict the impact of a crude-oil on foam based on the crude-oil composition.
- Our third question: does oil impact bulk-foam in the same way it impacts foam in porous media?
  - Our hypothesis is that some of the mechanisms in which oil impacts bulk-foam also occur in porous media.
  - Our third objective is to correlate the behaviour of foam in the presence of an organic compound (OC) in bulk and in porous media. This would allow one to make reliable predictions on the impact of an OC on foam in a porous medium based on the behaviour of bulk-foam in the presence of an OC.
- Our fourth question: what is the impact of solubilized oil on foam in porous media?
  - Our hypothesis is that some of the impact of (crude-) oil, in oleic phase, on foam in porous media is caused by the solubilized components.
  - Our fourth objective is to describe the impact of solubilized (crude-) oil on foam and to relate it to the impact of (crude-) oil, as a separate phase, on foam. It has been claimed that the effect of oils on foam directly reflects the effect of oil components solubilized in the surfactant solution.
- Our fifth question: is emulsion generated when both foam and oil flow through a porous medium?
  - Our hypothesis is that when oil and foam flow together through a porous medium an emulsion can be generated and this is reflected in the apparent viscosity.
  - Our fifth objective is to model three-phase co-injection of surfactant solution, gas and crude oil and to account for generated foam and emulsion. Currently foam models assume that only the gas mobility is reduced in the three-phase flow of surfactant solution, gas and oil. However, co-mingled flow of surfactant solution and crude oil can result in the generation of emulsion, and thereby result in a decreased oil and/or water mobility.
- Our fifth question: when crude-oil comes into contact with pre-generated foam, does the foam collapse immediately and if not over what distance is steady-state achieved?
  - Our hypothesis is that when pre-generated foam comes into contact with crude-oil, the foam weakens and the fluids have the same characteristics as with three-phase co-injection after flowing together for 0.15 m.

- Our objective is to develop a novel method to investigate the impact of crude oil on in-situ pre-generated foam. With this experimental method we aim to replicate the impact of crude oil on foam as it occurs when it is applied for EOR purposes.

1.4. Outline

In chapter 2 we investigate the correlation between the surfactant concentration of a surfactant solution injected into a porous medium and f_w^*. We find that, as surfactant concentration varies, the fraction of the surfactant molecules in the surfactant solution residing on the gas-water interfaces of foam is roughly constant at the f_w^*. We find that for surfactant solutions with a higher salinity a greater fraction of the available surfactant molecules occupy the gas-water interfaces. This suggests that the mechanism is related to the ability transport surfactant to and from gas-water surfaces as they stretch and contract moving through the pore space.

In chapter 3 we investigate the impact of a crude oil on foam in bulk and in a porous medium. In this study we also investigate if we can reproduce the impact of crude oil on foam with a simple oil mixture, with its composition based on the crude oil composition (from gas chromatography and its total acid and base number). We also find a correlation between the behaviour of foam in the presence of oil in bulk and in a porous medium.

In chapter 4 we delve deeper on the impact of crude oil and hexane on foam in a porous medium. We investigate if the impact of solubilized crude oil and hexane on foam in a porous medium can explain the impact of either crude oil or hexane, as a separate phase, on foam in a porous medium. We do this by co-injecting surfactant solution, gas, and in some cases oil as a separate phase into a core. In these experiments we control the fractional flow of all phases. By accounting for the impact of emulsion (generated in the porous medium) on liquid mobility and by accounting for the impact foam on the gas mobility, we can fit a simple model to our experimental data.

In chapter 5 we present a novel experimental method to investigate the impact of (crude) oil on in-situ pre-generated foam in a porous medium. This approach allows us to generate foam in absence of oil and then examine the effect of subsequent contact of crude oil, in a single porous medium. In this chapter we discuss the approach and analyse the results of our experiments. We see that foam apparent viscosity progressively decreases after its first contact with crude oil, and can weaken as much as 80% over a length of 0.10 m. This indicates that foam and oil reach steady-state almost instantaneously compared to the length of a reservoir-simulation grid-block. This study extends previous micro-model studies on the impact of (crude) oil on in-situ generated foam to conditions more like field application.

In chapter 6 we summarize the conclusions of this work and we give recommendations for further research on foam in porous media and the impact of crude oil on it.

Note from the author: this dissertation is based on paper published in or submitted to peer-reviewed journals. Therefore, some chapters of this dissertation have parts of overlapping text.

2. Effect of surfactant depletion by gas-water interfaces on foam stability in porous media

The content in this chapter is submitted to a journal for publishing: Hussain, A. A. A., Vincent-Bonnieu, S., Pilus, R. M. and Rossen, W.R. Effect of surfactant depletion by gas water interfaces on foam stability in porous media.

2.1. Introduction

Due to the costs of the surfactants, it is vital that the operator injects the appropriate concentration of surfactant into the reservoir. Injecting a surfactant solution with a lower surfactant concentration might lead to an unstable foam that makes the foam process inefficient. Conversely, increasing the surfactant concentration above a certain value might not lead to an improvement in the sweep efficiency, while negatively impacting the economics of the project.

Foam characteristics in a porous medium are a function of the gas volume fraction of the injected surfactant solution and gas, called *foam quality*. Ettinger and Radke (1992) observe that foam-bubble size is about the size of the pores for low-quality foam. Foam reaches its transition from the low-quality regime to the high-quality regime at the limiting capillary pressure (P_c^*). Foam stability is extremely sensitive to capillary pressure (and therefore water saturation) beyond this point. Foam bubbles collapse for P_c^* greater than P_c^*, and grow to become larger than pore bodies, in what is called the *high-quality* regime. As a result, as foam-quality increases beyond the transition value bubble size increases and gas mobility increases at nearly constant water saturation (Khatib et al., 1988). If the transition between regimes is abrupt, then at the transition P_c^*, bubble size is roughly equal to pore-body size. Figure 2.1 is a schematic of the trend of apparent viscosity as a function of foam quality (Boeije and Rossen, 2015; Jones et al., 2016a; Kapetas et al., 2015a). The apparent viscosity is defined as the viscosity of a hypothetical single-phase fluid which shows the same pressure gradient as the injected foam at a given superficial velocity.

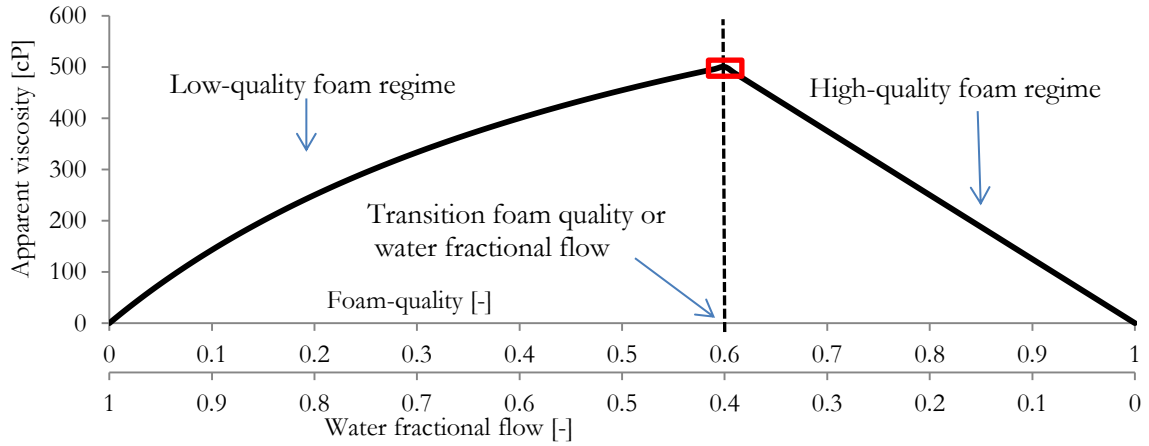

Figure 2.1: Schematic of trend of apparent viscosity as a function of foam quality or water fractional flow for foam injected into a porous medium at a fixed total injection rate of water and gas. Figure assumes an abrupt transition between regimes.

The effect of surfactant concentration on foam stability is well understood in bulk foam (i.e., outside porous media). The fundamental principle of the stability of bulk foam is that foam films are most stable when maximally covered by surfactant molecules (Manev et al., 1974). Moreover, after foaming, the surfactant concentration of the bulk solution should not have

decreased "too far" (Boos et al., 2012) below the critical micelle concentration (CMC) by depletion by the gas-water interface. In other words, foam stability, in bulk, reaches its maximum at a small multiple of the CMC. In porous media, foam apparent viscosity continues to increase with increasing surfactant concentration even far above the CMC. Foam-floods are performed usually with surfactant concentrations many times greater than the CMC (Farajzadeh et al., 2012; Khatib et al., 1988; Lee and Heller, 1990; M.G. Aarra and A. Skauge, 2000). Moreover, f_w^* decreases with increasing surfactant concentration (Apaydin and Kovscek, 2001; Eftekhari and Farajzadeh, 2017; Jones et al., 2016a; Kahrobaei and Farajzadeh, 2019; Lee and Heller, 1990). The effect of surfactant depletion at foam interfaces when generating bulk foam and emulsion has been studied (Boos et al., 2012; Tcholakova et al., 2004, 2003), but not, to date, its effect on foam in porous media.

In this study, we estimate the surfactant concentration necessary in the injectant to saturate the gas-water interfaces in flowing foam in porous medium at f_w^*. We do this with a simple material balance on surfactant flowing into and flowing out of a region behind the foam front. We assume the surfactant flowing into and out of the region behind the foam front is at equilibrium.

2.2. Material balance on surfactant behind foam front

Here we consider the adsorption of surfactant to gas-water interfaces and show that the surfactant concentration required to saturate the gas-water interface is a function of the flowing water fraction and not directly of water saturation.

Behind the foam front, i.e. within the foam bank, the saturation, fractional flow, bubble size and surfactant concentration are each uniform; see Figure 2.2. We consider a small incremental volume element in this foam bank. In this element surfactant adsorption on the solid interface is satisfied. The total surfactant concentration in the liquid is C_s. Some of the surfactant molecules are adsorbed to the gas-water interfaces ($C_{s,i}$) and some of the surfactant molecules are in the surfactant solution bulk ($C_{s,b}$), such that $C_{s,i} + C_{s,b} = C_s$. At steady-state, $C_{s,i}$ and $C_{s,b}$ are the same leaving as entering the element.

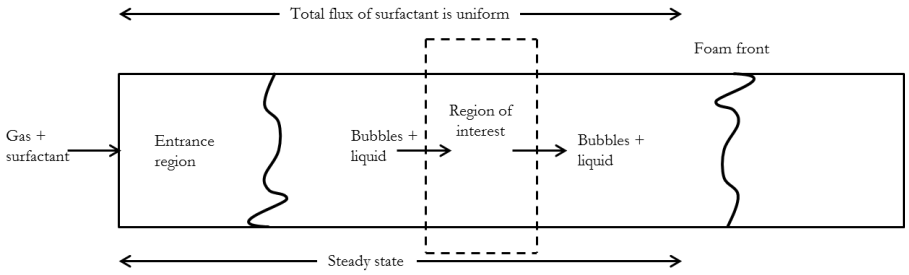

Figure 2.2: Schematic of foam propagating through a porous medium. We perform a material balance on surfactant in this region.

Let the bulk surfactant concentration of the foam flowing into the element be $C_{s,b}$. Resident fluid interacts with the flowing surfactant solution and foam. This means that at steady state $C_{s,b}$ in the resident liquid must be the same as in the flowing foam, i.e.

$$C_{s,b}^{in} = C_{s,b}^{out} = C_{s,b}^{res} \qquad \textbf{Eq. 2.1}$$

where $C_{s,b}^{res}$ is the concentration of surfactant dissolved in the liquid (i.e., not occupied at interfaces) within the volume element. Otherwise, surfactant would be transported (perhaps slowly) from the resident liquid to or from the flowing surfactant solution. Because of this interaction, surfactant concentration in the efflux would differ from the influx, and surfactant concentration in the control volume would change with time and thus not be at steady-state.

Therefore, in the foam leaving the element the concentration of surfactant in bulk liquid is $C_{s,b}$ and the surfactant depleted by the gas-water interface is $C_{s,i}$. The foam leaving the element transported with a water volume given by the water fractional flow, and this water must provide the surfactant needed for the bubbles also moving with the foam. Put another way, the concentration of surfactant in the liquid phase is determined by the fraction of surfactant in the flowing foam that is lost to interfaces in the flowing foam. Thus the fraction of surfactant in liquid lost to the gas-water interfaces is determined by water fractional flow, not water saturation per se as assumed by Jones et al. (2016)). With this finding, we can determine the surfactant depletion by the gas-water interface as a function of f_w^*.

2.3. Surfactant depletion by the gas-water interface

To investigate the surfactant depletion by gas-water interface ($C_{s,i}$), at the fractional flow f_w^*, we make the following assumptions for foam in the low-quality regime:

1. Each gas bubble is spherical. Peksa et al. (2015) make this simplifying assumption in their analysis of pore sizes in Bentheimer sandstone. See discussion of this point below.
2. The gas bubble radius equals the volume-average pore-body radius.
3. The surface area per surfactant molecule on a bubble surface is the same as on a flat surface.
4. The gas-water interface is saturated with surfactant molecules.

Our method for modelling the gas-water interfacial area of flowing gas in a porous medium is given by

$$A_f = f_g \times \frac{A_b}{V_b} = f_g \times \frac{4\pi {r_b}^2}{\frac{4}{3}\pi {r_b}^3} = f_g \times \frac{3}{r_b} \qquad \textbf{Eq. 2.2}$$

where A_f is gas-water interfacial area in a unit volume, A_b is the surface area of a gas bubble [m^2] V_b is the volume of a gas bubble [m^3], and r_b is a gas bubble radius [m]. f_g/V_b in Eq. 2.2 is the number of bubbles per unit volume. We model $C_{s,i}$ at f_w^* using a similar method to that applied by Boos et al. (2012) for bulk foam:

$$f_w^* \times C_{s,i} \times \rho_s = \frac{A_f^*}{A_s} = f_g^* \times \frac{A_b}{V_b \times A_s} = f_g^* \times \frac{3}{r_b \times A_s} \qquad \textbf{Eq. 2.3}$$

where A_s is the surface area covered by a unit mass of surfactant [m^2/kg] and ρ_s is the surfactant solution density [kg/m^3], and superscript * means the term is evaluated at the transition foam quality. The left side of Eq. 2.3 is the total mass of surfactant on interfaces per unit volume of

foam. f_g^*/V_b is the number of bubbles per unit volume at f_g^*, and A_b/A_s is the mass of surfactant on the interface of a bubble. We rearrange Eq. 2.3 with $f_w^* = 1 - f_g^*$ as

$$f_w^* = (1 - f_w^*) \times \frac{3}{r_b \times A_s \times C_{s,i} \times \rho_s} \quad \text{Eq. 2.4}$$

to solve for f_w^* we rearrange Eq. 2.4 as

$$f_w^* \times r_b \times A_s \times C_{s,i} \times \rho_s = 3 - 3 \times f_w^* \quad \text{Eq. 2.5}$$

and rearrange Eq. 2.5 as

$$f_w^* \times \left(3 + r_b \times A_s \times C_{s,i} \times \rho_s\right) = 3 \quad \text{Eq. 2.6}$$

and then rearrange Eq. 2.6 as

$$f_w^* = \frac{3}{3 + r_b \times A_s \times C_{s,i} \times \rho_s} \quad \text{Eq. 2.7}$$

By describing $C_{s,b}$ as a multiple Z of $C_{s,i}$, i.e.

$$C_{s,i} + C_{s,b} = C_{s,i} + Z \times C_{s,i} = C_s \quad \text{Eq. 2.8}$$

we can define f_w^* as a function of C_s by plugging Eq. 2.8 in Eq. 2.7:

$$f_w^* = \frac{3}{3 + r_b \times A_s \times \frac{C_s}{Z+1} \times \rho_s} \quad \text{Eq. 2.9}$$

2.4. Experimental materials and methods

We correlate the surfactant concentration and f_w^* calculated with experimental data from work of Kahrobaei and Farajzadeh (2019), Eftekhari and Farajzadeh (2017) and Jones et al. (2016). Table 2.1 summarises the experimental conditions.

Table 2.1: Experiment conditions of Jones et al. (2016) and Eftekhari and Farajzadeh (2017).

	T [°C]	Back pressure [bar]	Water composition	Velocity [m/day]	Core material / diameter [m]
Kahrobaei and Farajzadeh (2019)	30	25	1 wt.% NaCl	1.22	Bentheimer sandstone / 0.038
Eftekhari and Farajzadeh (2017)	22	95	Demi water	1.22	Bentheimer sandstone / 0.038
Jones et al. (2016)	60	20	Exp A: 3 wt.% NaCl Exp B: "7 Salts solution" (2.5 wt.% NaCl and 1.0 wt.% other salts, incl. Ca^{2+} and Mg^{2+})	2.06	Bentheimer sandstone / 0.0094

The experiments were conducted by co-injecting surfactant and gas, at various ratios, in a vertically oriented core. The data were collected after the experiments reached steady-state in pressure-gradient. The pressure gradients were determined over a section some distance downstream from the inlet and some distance upstream from the outlet.

The experiments by Kahrobaei and Farajzadeh (2019) were conducted in a single core and their surfactant solutions contained 1.0 wt.% NaCl. After conducting several experiments with a surfactant solution with a fixed surfactant concentration, they flushed the core with isopropyl alcohol. The core was subsequently flushed with CO_2 and then vacuumed before starting experiments at another surfactant concentration. We obtained the f_w^* values from the trend of the data by Kahrobaei and Farajzadeh (2019).

The experiments by Eftekhari and Farajzadeh (2017) were conducted in a single core and with decreasing surfactant concentration. They flushed the core with isopropyl alcohol after every experiment to kill the foam, followed by several pore volumes of water to displace the alcohol. In their experiments, they used demineralized water for their surfactant solution, which can cause clay minerals to swell (Mungan, 1965), and thus might result in a different pore-size distribution than for the experiments conducted by Kahrobaei and Farajzadeh (2019) and Jones et al. (2016). We obtained the f_w^* values from the trend of the data by Eftekhari and Farajzadeh (2017).

The experiments by Jones et al. (2016) were conducted in cores of narrow diameter (0.0094 m, vs 0.038 m for Kahrobaei and Farajzadeh (2019) and Eftekhari and Farajzadeh (2017)). They flooded the porous medium with several pore-volumes of each solution prior to the start of each experiment and did not use alcohol in their experiments. Jones et al. (2016) conducted experiments with two surfactant solutions: solution A consisted of 3 wt.% NaCl and solution B consisted of 2.5 wt.% NaCl and 1.0 wt.% of six other salts, including $MgCl_2$ and $CaCl_2$; see Jones et al. (2016) for a more detailed overview of their solutions. Because Jones et al. (2016) observe a sharp transition between the low- to high-quality regimes, we determined f_w^* from their experimental data.

2.4.1. Surface area covered by a single surfactant molecule

To estimate the surface coverage of surfactant, we use Table 2.2-a, after Tuvell et al. (1978), which gives the average gas-water interfacial area per surfactant molecule for Alpha-Olefin Sulfonate (AOS) surfactants at 23°C. $C_{14/16}$ AOS is the surfactant mixture used in the experiments discussed in this work (Eftekhari and Farajzadeh, 2017; Jones et al., 2016a; Kahrobaei and Farajzadeh, 2019). Tuvell et al. (1978) made their measurements in solutions with salinities up to 0.0125 wt.% (3/2 mixture of Ca^{2+}/Mg^{2+}). When fitting our model to the data by Kahrobaei and Farajzadeh (2019) and Eftekhari and Farajzadeh (2017) we assume the surface area per surfactant molecule is equal to that measured by Tuvell et al. (1978), 40.7 $Å^2$. This is because we lack data on interfacial tension as a function of surfactant concentration under the experimental conditions of Kahrobaei and Farajzadeh (2019) and Eftekhari and Farajzadeh (2017), which is necessary to calculate the surface area per surfactant molecule. We calculate the average surface area per surfactant molecule for the experiments by Jones et al. (2016) using the Gibbs equation, $\Gamma = -1/RT\ (\partial\gamma/\partial \ln C_{surf})_T$ (Rosen, 2004; Tuvell et al., 1978), where Γ is the area per mole of surfactant, R is the gas constant [J/K·mol], T is the temperature [K] and γ is the surface tension [mN/m]. See Table 2.2-b for the calculated area per surfactant molecule. Jones et al. (2016) measured a CMC value of 0.002 wt.% at a temperature of 60°C for both their solutions.

Kahrobaei and Farajzadeh (2019) measured it to be at 0.008 wt.% at room temperature and Eftekhari and Farajzadeh (2017) measured it to be 0.08 wt.% at room temperature.

Table 2.2: On the left: Surfactant Area/Molecule (Å²) at the air/water interface, measured at a temperature of 23°C, after Tuvell et al. (1978). On the right: Surfactant Area/Molecule (Å²) at the air/water interface, calculated with the surface tension measurements by Jones et al. (2016), at a temperature of 60°C.

a

	Water hardness as $CaCO_3$ – 3/2 Ca^{++}/Mg^{++}		
Surfactant	0 wt.%	0.0050 wt.%	0.0125 wt.%
C_{14} AOS	42.8		39.9
C_{16} AOS	34.9		28.7
2/1 blend – C_{14}/C_{16} AOS	-	40.7	31.6

b

	Aqueous solution	
Surfactant	3 wt.% NaCl	7 Salts solution, (2.5 wt.% NaCl and 1.0 wt.% others)
C_{14} AOS	-	-
C_{16} AOS	-	-
2/1 blend – C_{14}/C_{16} AOS	50.7	45.8

2.4.2. The bubble size of low-quality foam in a porous medium

The total gas-water interfacial area of foam in porous media depends on the bubble size. However, the radius of flowing foam bubbles in a 3-dimensional porous medium is unknown. For foam in the low-quality regime, many researchers assume that the bubble size is equal to the average pore size (Alvarez et al., 2001; Bertin et al., 1998; Ettinger and Radke, 1992; Gido et al., 1989; Mast, 1972); others assume twice the pore size (Shi et al., 2016; Tang and Kovscek, 2006), and some a third of the grain size in an unconsolidated sand-pack (Kam and Rossen, 2003). Some of these assumptions were made based on experiments measuring the bubble size at the outlet of the core. In this chapter we assume the average foam bubble radius is equal to the volume-average pore-body radius.

Bentheimer sandstone is considered relatively homogenous and poor in clay content (Peksa et al., 2015). To determine the pore-body-diameter distribution of Bentheimer sandstone Peksa et al. (2015) first determine the volume of each pore. Then they calculate the "effective" pore-body diameters with the same volumes as the actual pores. Figure 2.3-a shows the distribution of pore-body diameters for Bentheimer sandstone and Figure 2.3-b shows the distribution of pore-throat diameters, determined from micro-CT images with a resolution of 5 μm (Peksa et al., 2015). Based on their data we find that the volume-average pore-body diameter is 0.295 mm. A sphere of course has the minimum surface area/volume ratio of any pore shape, so we believe by using the equivalent sphere calculated by Peksa et al., and assuming a spherical bubble shape in Eq. 2.7, gives a conservative estimate of the actual surface area of bubbles each occupying a pore in the porous medium.

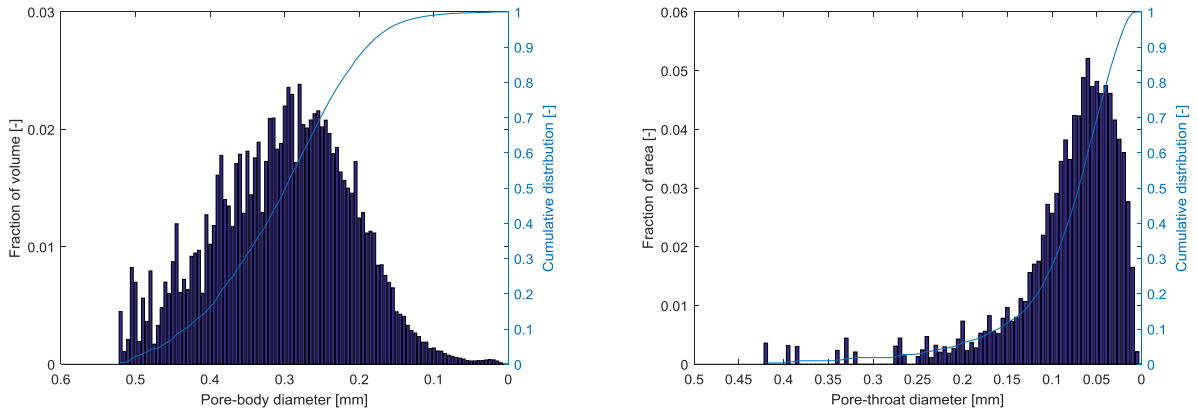

a b

Figure 2.3: a: pore-body diameter distribution of Bentheimer sandstone. b: pore-throat diameter distribution of Bentheimer sandstone, after Peksa et al. (2015).

2.5. Results and discussion

Figure 2.4 shows f_w^* as a function of C_s, using the data of Kahrobaei and Farajzadeh (2019), Eftekhari and Farajzadeh (2017) and Jones et al. (2016). Figure 2.4 also shows the fit of Eq. 2.9 to the experimental data. Figure 2.5 shows f_w^* vs. the fraction of surfactant in the injectant residing on the gas-water interface ($C_{s,i}/C_s$). Here we see that foam with more than 10% of the available surfactant residing on the gas-water interface was observed only with a surfactant concentration of 0.1 wt.% or less in the injectant. The foams with the largest fraction of surfactant residing on the interface had both NaCl and divalent ions in the solution, and the foams with the smallest fraction of surfactant residing on the interface were made with surfactant in demineralized water.

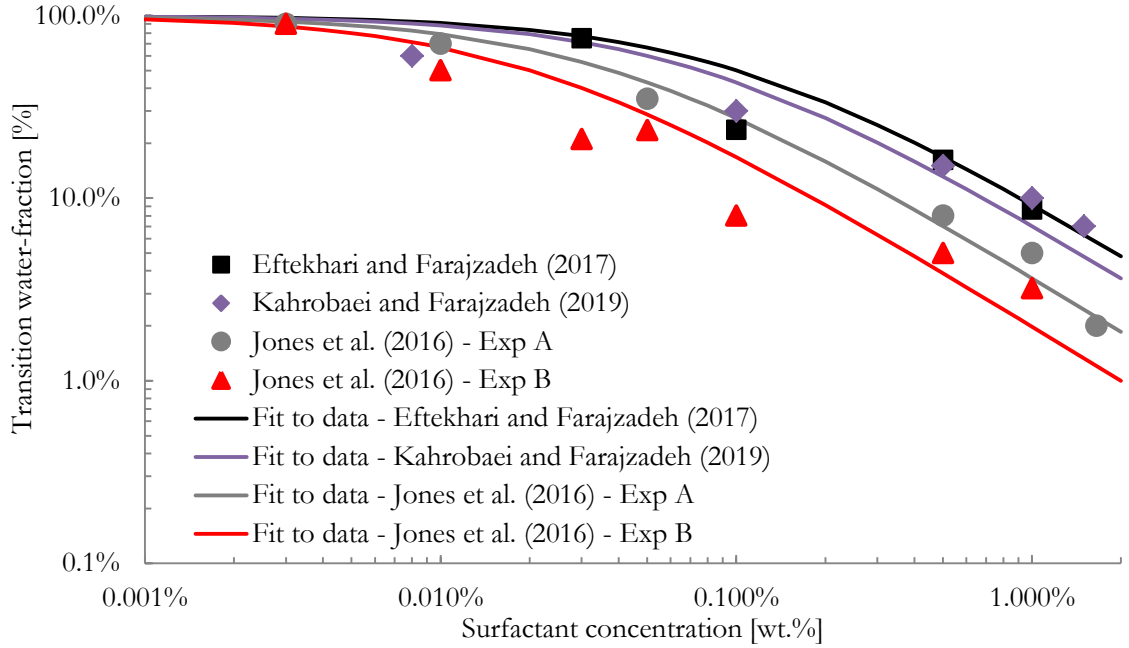

Figure 2.4: Experimental data and fits of f_w^* as a function of surfactant concentration. Experimental data after Eftekhari and Farajzadeh (2017), Kahrobaei and Farajzadeh (2019) and Jones et al. (2016) and. For the data fits we use Z = 97, 73, 36, 19 to fit the experimental data by Eftekhari and Farajzadeh (2017), Kahrobaei and Farajzadeh (2019), Jones et al. (2016) series A and series B respectively.

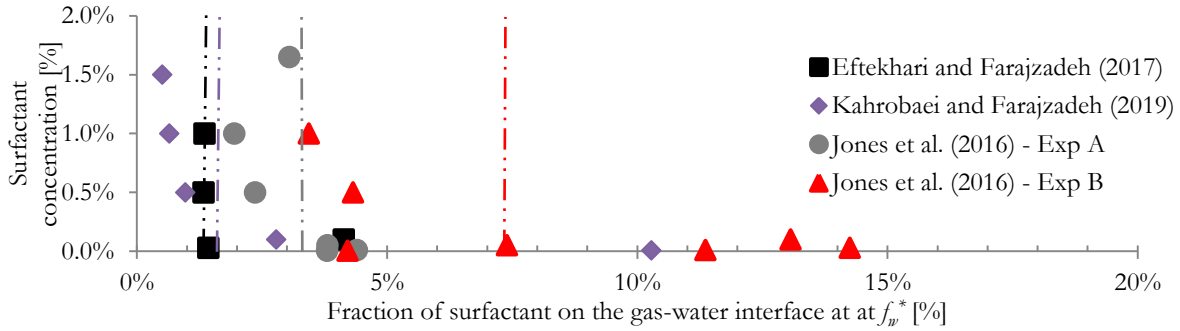

Figure 2.5: Surfactant concentration vs the fraction of the available surfactant residing on the gas-water interfacial area, at the f_w^*. Experimental values after Kahrobaei and Farajzadeh (2019), Eftekhari and Farajzadeh (2017) and Jones et al. (2016). The vertical lines are equal to 1/(1+Z).

This can be explained by the impact of salinity on both the critical capillary pressure, above which foam films collapse, and on surfactant dynamics. With respect to the impact of salinity on the critical capillary pressure, Khristov et al. (1983) show that the critical capillary pressure increases with increasing salinity. It is believed that increasing critical capillary pressure reduces f_w^* (Khatib et al., 1988), and thereby results in a higher fraction of the surfactant on the gas-water interface at f_w^*.

Concerning the impact of salinity on surfactant dynamics: as foam moves through pores, the lamellae stretch and contract, and thus the local gas-water interfacial area changes continuously (Jiménez and Radke, 1989). Jiménez and Radke (1989) show that water transport must be fast enough into stretching lamellae to prevent them from thinning below the minimum film thickness and thereby reaching the critical capillary pressure. We believe there is a similar mechanism of surfactant transport from the bulk solution to stretching gas-water interfaces to stabilize foam in porous media. Faster movement of surfactant molecules to the gas-water interface can be achieved by increasing the surfactant concentration and NaCl concentration (Rosen, 2004; Rosen and Hua, 1988). Moreover, Mg^{2+} and Ca^{2+} ions have a more pronounced impact than NaCl on accelerating the transport of a sodium dodecyl sulfate (SDS) from solution to the interfaces (Fainerman et al., 2012). This can explain why the largest fraction surfactant was depleted with the surfactant solution containing NaCl, Mg^{2+} and Ca^{2+} ions: a smaller excess is needed in bulk to transport surfactant to stretching lamella. This can also explain why foams formed with surfactant in demineralized water had the smallest fraction of the surfactant depleted by the gas-water interface.

Kapetas et al. (2015) conducted similar experiments to those of Kahrobaei and Farajzadeh (2019), Eftekhari and Farajzadeh (2017) and Jones et al. (2016), at various temperatures between 20°C and 80°C. In his experiments the difference in temperature has a limited impact on f_w^* and S_w^*. Therefore, we neglect the impact of temperature in our analysis.

It is unclear why foams with the highest fraction of surfactant adsorbed on the gas-water interface at f_w^* were made with the surfactant solutions with lowest surfactant concentration.

As discussed above, the method applied by Peksa et al. (2015) to determine to pore-size distribution of Bentheimer sandstone likely underestimates the ratio of pore-body surface area to volume. Because we use their numbers as an input in our analysis, we underestimate the average surface area per foam bubble and thereby underestimate the surfactant depletion by the gas-water interfaces. Therefore, our estimated $C_{s,b}/C_{s,i}$ ratio is likely to be greater than the actual ratio.

2.6. Modelling the impact of surfactant concentration on foam behaviour

Kahrobaei and Farajzadeh (2019) and Jones et al. (2016) show that surfactant concentration in the injectant does not impact foam behaviour in the low-quality regime. Moreover, they argue that the impact of surfactant concentration on foam in porous is not properly captured in commercial simulators.

With our model of surfactant depletion, we can qualitatively match the surfactant concentration effect on f_w^* (Figure 2.4). Thus, the foam model can be improved by including a new function of surfactant concentration, as shown with the solid lines in Figure 2.4, which is based on the ratio $C_{s,b}/C_{s,i}$, Z (Eq. 2.9).

2.7. Conclusions

We propose a simple model to estimate surfactant depletion by the gas-water interface at the transition water-fraction (f_w^*). We find that the fraction of surfactant depleted by the gas-water interface can be as much as 14% of the available surfactant in the injected liquid. Given the simplifying assumption of bubble and pore shape made, our values are likely to be underestimates.

We find that for a given salinity and surfactant formulation surfactant depletion by the gas-water interface at f_w^* is roughly proportional to the surfactant concentration in the injectant.

Foams made with higher-salinity solutions, which increase the critical capillary pressure for foam-film stability and speeds the movement of surfactant molecules to the gas-water interface, can allow a greater depletion by the gas-water interface. Thus in these cases a higher salinity resulted in a lower f_w^* at the same surfactant concentration. The connection between salinity and surfactant dynamics suggests that an excess of surfactant is required to provide rapid transport of the surfactant to the gas-water interface. This mechanism is similar to the mechanism proposed by Jiménez and Radke (1989) for water transport to stretching film lamellae.

This work suggests an important connection between surfactant adsorption at gas-water interfaces and foam behaviour in porous media even far above the CMC. More work is needed to properly model the surfactant mass-transfer process in foam in porous media.

Conclusions

3. Impact of different oil mixtures on foam in porous media and in bulk

This chapter is based on the paper Hussain, A. A. A., Vincent-Bonnieu, S., Kamarul Bahrim, R.Z., Pilus, R. M. and Rossen, W.R., 2019, Impact of different oil mixtures on foam in porous media and in bulk. Journal of Industrial and Engineering Chemistry Research

3.1. Introduction

Currently, to understand and model the behaviour of foam in an oil reservoir, experiments need to be conducted in the presence of the specific crude oil in a porous medium, and extrapolating from one crude oil to another is not possible. This can be a time-consuming process. It is therefore desirable to model the impact of a crude oil on foam solely based on the crude oil composition. This would allow one to efficiently screen reservoirs for foam application.

To date there isn't a published model which can predict the impact of a crude oil on a foam from the crude-oil composition based on gas chromatography (GC), its total acid number (TAN) and total base number (TBN), or its saturate, aromatic, resin and asphaltene (SARA) fractions. There are various reasons why it is difficult to make such a model. These include scarcity of data on oil composition, countless different compounds in the crude oil (Speight, 2014), and some compounds weakening and others stabilizing foam (Vikingstad et al., 2005). Here we create a "synthetic" crude oil from seven pure organic compounds (OC). Its composition is based on the most prevalent components of the actual crude oil, its TAN and TBN, and an organosulfur concentration common in "sweet" crude oils.

Previous attempts to relate the impact of crude oil on foam focused on the SARA content. Jensen and Friedmann (1987) conducted steam-foam experiments in porous media in the presence of four different crude oils, and they found that the pressure drop across their core was a function of only the oil saturation, irrespective of the crude oil. Pu et al. (2017) and Vikingstad et al. (2005) conducted bulk-foam experiments with different crude oils, and observed that the different crude oils impacted their foams differently. However, they did not find an obvious relationship between the SARA composition of their crude oils and the impact on their bulk foam.

Others have examined the impact of different pure compounds present in crude oils (alkanes, organic acids, alcohols, and aromatics) on foam in bulk and in porous media (Dalland et al., 1994; Laskaris, 2015; Osei-Bonsu et al., 2017; Tang et al., 2018; Vikingstad et al., 2005; Zhang et al., 2003). Tang et al. (2018) co-injected different pure alkanes (C_{16}, C_{10}, C_8, C_6) with foam in a sandstone, however none resulted in an apparent viscosity as low as we observed with our crude oil, see below. Moreover, it is not clear how the impact of pure oils on foam relate to the impact of crude oils or oil mixtures on foams in bulk and in porous media.

Here we look at how OCs, pre-dispersed (as a separate phase) in the surfactant solution, impact bulk foam generation and collapse; i.e. we investigate the anti-foaming properties of different pure OCs (Pugh, 1996). The anti-foaming impact of an OC can be different from the de-stabilization by an OC scattered over an already-formed bulk foam (i.e., de-foaming), which is tested in other studies (Simjoo et al., 2013). An anti-foamer ruptures foam films in two steps; the OC drop first enters the air-water interface, after which it spreads over the foam film, causing it to rupture (Pugh, 1996). The foamability of the foam can be reduced by OC drops, as they induce foam bubbles to coalesce during foam generation (Arnaudov et al., 2001). Moreover,

natural cationic surfactant in the crude oil can react with anionic surfactant of the foaming solution, leading to a larger aggregate without a hydrophilic head which is often not water-soluble (Antón et al., 2008). Surfactant solution and an OC can also form high-viscosity emulsions which stabilize bulk foam (Koczo et al., 1992).

A benefit of bulk-foam experiments is that the different ways in which an OC impacts foam can be observed visually. In contrast, with foam in an opaque porous medium only the pressure gradient and the saturation of the different phases can be determined. Although the effluent from the porous medium can be inspected visually for clues on the foam characteristics in the porous medium, it does not necessarily reflect the foam characteristics in the porous medium, e.g. due to foam generation at the outlet by the capillary end effect. Foam behaviour in the presence of an OC isn't necessarily the same in bulk and in a porous medium. Jones et al. (2016b) showed a strong correlation between maximum apparent viscosity of foam in a porous medium and bulk-foam half-life for foam in absence of oil but a weak correlation for foam in presence of oil. However, we believe conducting both porous-media experiments and bulk-foam experiments gives more information on how foam interacts with an OC in a porous medium. We do not consider here the interfacial tensions (IFT) between OC, surfactant solution, and gas. It has been shown that foam-stability predictions based on IFT values are unreliable, both in bulk and in porous media (Mannhardt et al., 1998; Vikingstad et al., 2005).

With this study we investigate two screening methodologies: forecasting the impact of a crude oil on a foam based on the crude oil composition and forecasting the impact of an oil on foam in a water-wet porous medium based on bulk-foam experiments. To relate the impact of a specific crude oil on foam to the crude oil composition we assemble a synthetic crude oil, with its composition based on the GC analysis, the TAN and TBN of the crude oil. We also include an organosulfur in the synthetic crude oil because it is a common component of crude oils (Speight, 2014). For this study we assume that the composition of the crude oil defines how it impacts foam, both in bulk and in porous media. We conduct both bulk-foam experiments and porous-media experiments and investigate different ways to correlate the results.

In the next section we describe the materials used in our experiments and the experimental procedures. This is followed by a section with the experimental results and discussion, and finally we give the conclusions and recommendations based on our findings.

3.2. Material and procedures

Table 3.1 outlines our brine composition in mass per volume, which we used to make our surfactant solution, using the surfactant Alpha Olefin Sulfonate $C_{14/16}$ (AOS). The surfactant concentration was set to 0.5 wt.% AOS, which is more than 100 times the CMC value (Jones et al., 2016a).

Table 3.2 lists relevant physical and chemical properties of these components, and their fraction in the synthetic crude oil. Its composition is based on the crude oil's GC analysis, TAN and TBN. Although we do not know the sulphur content of the crude oil, we include an organosulfur compound in our synthetic crude oil at a concentration common in "sweet" crude oils (Mitra-Kirtley et al., 1998; Speight, 2014). N-octane (nC8) and hexadecane (C16) were used to represent the lighter and heavier alkanes in the crude. Toluene, dimethyl sulfoxide (DMSO), methyl cyclohexane (MCH), oleic acid (OA), octanoic acid and 1-octanol were used to represent

the aromatics, the cycloalkanes, organosulfur compounds, organic acids and organic bases, respectively, in the crude oil.

Table 3.1: Brine composition

Ions	Concentration (mg/l)
Na^+	11250
K^+	353
Mg^{2+}	1214
Ca^{2+}	400
Cl^-	20000
SO_4^{2-}	2593

We investigate the impact of the pure OCs on bulk foam and of pure n-octane and hexadecane on foam in porous medium. We also investigate the impact of the OCs in mixtures with the alkanes. To investigate the impact of OCs at concentrations in line with the crude-oil composition, we conducted experiments with a 50/50 vol.% n-octane/hexadecane mixture to which we added one other OC. See Table 3.2 for the concentration of the additives in the alkane mixture. We also conducted foam experiments in bulk and in a porous medium with the synthetic crude, using oleic acid as the organic acid.

Table 3.2: Physical and chemical properties of oil components at 25°C (Chumpitaz et al., 1999; Kirk-Othmer, 2004; Lide, 2015).

Component	Vol. fraction in synthetic crude oil	Purity	Molecular Weight (gram)	Specific gravity (-)	Viscosity (mPa·s)	Surface tension (mN/m)
n-Octane (nC8)	0.4467	99%	114.230	0.702	0.537	21.1
Hexadecane (C16)	0.4467	99%	226.440	0.773	3.545	27.1
Toluene (Tol)	0.05	99.8%	92.140	0.867	0.582	27.9
Dimethyl Sulfoxide (DMSO)	0.005	99.9%	78.130	0.845	0.286	42.9
Methyl Cyclohexane (CyclC6)	0.05	99%	98.190	0.771	0.727	23.3
Oleic acid (OA)	0.00086	99%	282.468	0.894	37.070	32.8 (at 20°C)
1-Octanol (C8-ol)	0.00074	99%	130.23	0.83	7.36	26.4
Octanoic acid[1]	0.00044	99%	144.21	0.907	5.74	23.7 (at 20°C)

[1]*Octanoic acid was only used to investigate its impact on bulk foam, separately and mixed with the alkane mixture.*

We conducted our bulk-foam experiment with 25 ml tubes, filled with 5 ml surfactant solution, and when testing the impact of an OC on foam, also 1 ml of OC. The bulk-foam experiments were conducted at ambient conditions. For each experiment we put four test tubes in a rack, with one tube filled only with 5 ml surfactant solution, as a benchmark. We shook the tube rack 20 seconds manually, and measured the foam volume, total liquid volume, and, if possible, the OC volume over time. By looking at the initial foam volume we gained information

on the foaming capacity in the presence of a specific OC. The time until foam volume has reached half its initial volume (half-life) gives information on foam stability. We stopped the experiment after the foam volume has reached half its initial value or at the latest after 300 minutes, except for the experiment with crude oil, which was stopped after 120 minutes. Bulk-foam experiments conducted in this way are much faster than detailed foam-column tests of the Ross-Miles test, and give qualitatively similar results (Drenckhan and Saint-Jalmes, 2015). We checked our results for consistency both by the inclusion of the benchmark sample without oil in each rack and by conducting two experiments with each oil additive.

Our experiments in a porous medium were conducted in a Bentheimer sandstone core, with 0.01 m diameter and 0.22 m length. The reported apparent viscosities are calculated from pressure measurements over a section which is 0.07 m in length, 0.05 m downstream from the inlet and 0.10 m upstream from the outlet. By water-flooding the core we determined the average permeability of the core to be $2.0 \pm 0.2 \times 10^{-12}$ m^2 and the permeability of the 0.07 m section of interest to be $2.2 \pm 0.2 \times 10^{-12}$ m^2. The set-up is similar to the one used by Jones et al. (2016b). We used two piston pumps to control our surfactant and OC injection. Nitrogen gas was supplied from a cylinder and connected to a mass-flow controller. The backpressure regulator is set at 40 bars. The core-holder was put into an oven at 30°C. The combined flow rate of OC, surfactant solution and gas was set at 0.1 ml/min (6.75 ft./day or 2.04 m/day). The OC fractional flow was set to 1% in all experiments, and the surfactant solution and gas fraction were varied. We co-injected OC with our surfactant solution and gas so that we could control the steady-state at which we collected our data. Without co-injecting OC, we could otherwise enter into the cycle of foam recovering some of the oil, resulting in stronger foam and greater capillary number, which in turn results in a lower oil saturation, and so on (Jensen and Friedmann, 1987).

3.3. Results and discussions

Bulk foam in the absence of OC has an initial volume of 9 ml and a half-life longer than 300 minutes (Figure 3.1). In the porous medium we find that apparent viscosity can be as high as 1500 cP, and is 1002 cP at 70% gas fraction (Figure 3.2). We consider this foam to be stable. Bulk foam generated in the presence of crude oil has an initial volume of about 2 ml, and a half-life exceeding 2 hours (after which we stopped the experiment). When co-injecting surfactant, gas and 1 vol.% crude oil, we find the apparent viscosity to be about one-tenth of that without OC (114 cP) (Figure 3.2).

Both hexadecane (C16) and n-octane (nC8) weaken foam in the porous medium and in bulk, reducing the initial foam volume, half-life, and apparent viscosity in the porous media, though not as severely as crude oil; see Figure 3.1-a, Figure 3.1-b and Figure 3.2. The apparent viscosity observed with 70%-quality foam and nC8 (217 cP) is of roughly the same magnitude as with crude oil (114 cP), which is much less than what we observed with 70%-quality foam and C16 (782 cP). Surprisingly, the apparent viscosity of 70%-quality foam with our C16/nC8 (633 cP) mixture is greater than the average of the apparent viscosities with 70%-quality foam and C16 and with nC8. This shows that the impact of an OC mixture on foam is not necessarily the average of the impact of its components, or skewed towards its most damaging component(s), as was observed with oleic acid (Tang et al., 2018a); see Figure 3.3. Thus, even if one knows how the constituents of an OC mixture impact foam separately, correctly predicting the impact of a mixture of those OCs on foam is not obvious.

With pure oleic acid (OA) and with OA at 0.1 vol.% in the alkane mixture, we observe a smaller initial foam volume in bulk and a shorter half-life, similar to what we observe with crude oil (Figure 3.1-a and Figure 3.1-b). However, the impact of the alkane mixture on bulk foam is not changed by the addition of 0.008 vol.% OA, a concentration which is in line with the TAN of the crude oil. At 0.008 vol.% OA in the alkane mixture, we observe a greater fluctuation in the apparent viscosity of 70%-quality foam than without OA in the alkane mixture (Figure 3.2). It is not immediately clear what physical phenomena occur in the porous medium causing the larger fluctuation in pressure readings. We also conduct bulk-foam experiments with octanoic acid, which has the same pKa as oleic acid, but has a shorter aliphatic chain compared to oleic acid (8 carbons vs. 18 carbon atoms). Pure octanoic acid reduces the initial foam volume and half-life (Figure 3.1-a and Figure 3.1-b). However, the bulk foam generated in the presence of the alkane mixture with octanoic acid has a longer half-life and larger initial volume than foam generated in the presence of the alkane mixture with oleic acid. This demonstrates that the aliphatic chain length of an organic acid plays a role in its impact on bulk foam. Zhang et al. (2003) Zhang et al. (2003) demonstrate that a mixture of hexadecane and 10 wt.% oleic acid weakens foam. This is facilitated by formation of small solid soap particles, formed by reaction of oleic acid with the calcium ions in the water, which reside on the hexadecane-drop surfaces. It is possible that we formed small solid soap particles with the organic acid and calcium ions in our solution (Table 3.1); however, we did not check for the presence of soap particles in our experiments. Our findings show that the impact of organic acid, and possibly present calcium soap particles, do not play a dominant role in how our crude oil impacts foam, in line with the observations by Vikingstad et al. (2005).

Our alkane mixture with octanol, which represents organic bases in the crude oil, has a similar impact on bulk foam as our alkane mixture with oleic acid, which represents the organic acids in the crude oil. However, in porous media, the impacts of the alkane mixture with and without octanol are not significantly different. This indicates that alcohols and organic bases in this crude oil do not play a significant role in the weakening of foam in porous media.

Pure methylcyclohexane (MCH) significantly reduces the half-life and the initial bulk foam volume. The bulk foam generated in the presence of the alkane mixture with MCH has a smaller initial volume, but longer half-life, than foam generated in the presence of the alkane mixture without MCH. The alkane mixtures with and without MCH do not impact foam in porous media significantly differently. This indicates that cycloalkanes of this crude oil do not play a significant role in the weakening of this foam in porous media.

The alkane mixture with toluene resulted in a slightly smaller initial bulk foam volume (7 ml) than the alkane mixture without toluene (8 ml), but a longer half-life (300+ min vs 133 min) (Figure 3.1-a and Figure 3.1-b). However, the apparent viscosities achieved with the alkane mixture with and without toluene were not significantly different. Because the molecular structure of toluene and MCH are so similar, it is surprising that the impact of toluene on bulk foam resembles the impact of hexadecane while the impact of MCH on bulk foam resembles that of n-octane. These experimental results indicate that simple aromatics and cycloalkanes, such as toluene and MCH, do not play a significant role in the impact of the crude oil on foam. Based on these experiments, however, we cannot say how a larger molecule, with multiple benzene rings, would impact foam, in bulk or porous media.

In our bulk-foam experiments with dimethyl sulfoxide (DMSO), it is completely soluble in the aqueous solution and does not impact the initial bulk foam volume and half-life. A smaller

initial bulk foam volume is generated in the presence of DMSO in the alkane mixture (6 ml) than in the presence of the alkane mixture without additives (8 ml). However, this foam has a longer half-life than foam generated in the presence of the alkane mixture without DMSO (300+ min vs 133 min). For foam in the porous medium, there is no significant difference between the apparent viscosity achieved in the presence of the alkane mixture with and without DMSO. This indicates that such organosulfur compounds in crude oil, at least by themselves, do not play a significant role in the interaction between foam and crude oil in a porous medium.

Comparing the impact of synthetic crude oil on foam to the impact of the alkane mixture on foam, we see a 15% smaller initial bulk foam volume, but a 40% longer foam half-life (Figure 3.1-a, Figure 3.1-b). In a porous medium we see a 20% lower apparent viscosity (Figure 3.2-a and Figure 3.2-b). The longer bulk foam half-life could be caused by the presence of MCH, DMSO, toluene, OA or Octanol. The apparent viscosity of 70%-quality foam in presence of synthetic crude (493 cP) is significantly greater than in the presence of the crude oil (114 cP). These experiments indicate that our synthetic crude oil does not impact foam (in bulk or porous media) like the crude oil, even though the synthetic crude-oil composition is based on the crude-oil composition.

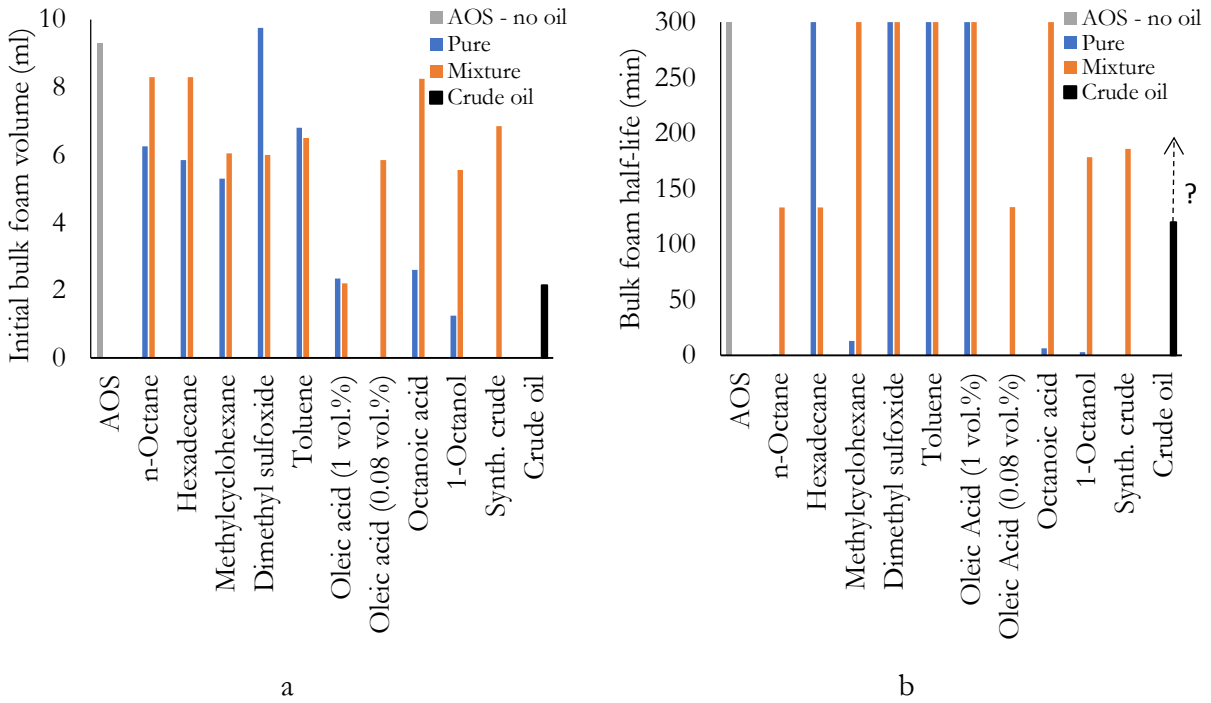

Figure 3.1: a) initial bulk-foam volume generated with AOS surfactant in the presence of different pure OC or alkane mixtures with an additive. b) time until the bulk foam volume collapsed to half its initial volume, i.e. the foam half-life, in the presence of different pure OC or alkane mixture with additive. Note that all the given values are the average values obtained over two experiments and that the experiment with crude oil was stopped after 120 minutes.

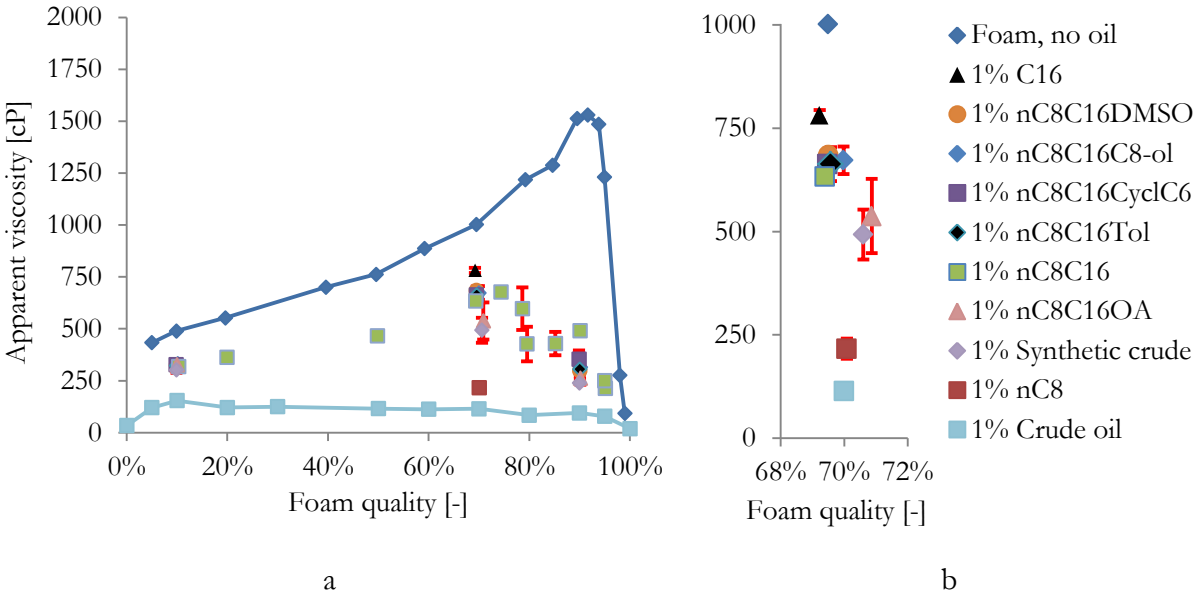

a b

Figure 3.2: a) the apparent viscosities in the porous medium, as a function of foam quality, for foam in absence of OC and in the presence of a pure OC or OC mixture at 1% fractional flow. Legend is at the far right. b) The same data, but only over a range of foam quality between 68% and 72%. For foam without OC, we observed an apparent viscosity of 1002 cP at 69% foam quality.

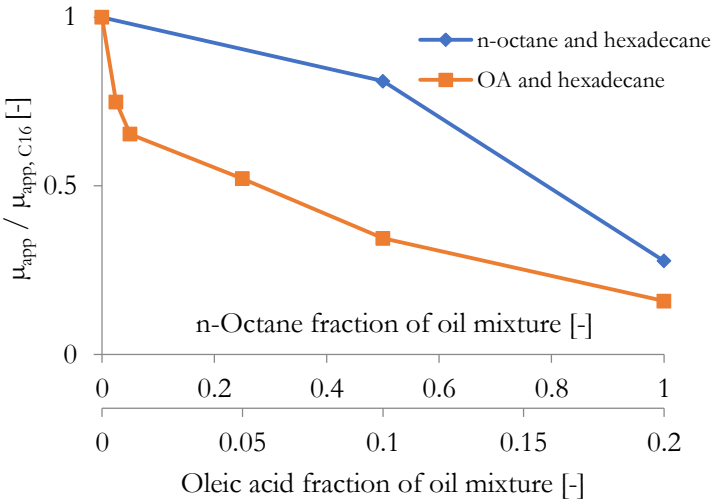

Figure 3.3: Ratio of apparent viscosity observed with an OC mixture to the apparent viscosity observed with pure hexadecane, as a function of the n-octane and OA fraction in a mixture with hexadecane. The experimental data for apparent viscosity in the presence of a mixture of oleic acid and hexadecane are from Tang et al. (2018). The lines are to guide the eye.

It would be useful to be able to forecast foam behaviour in porous media based on bulk-foam experiments due to the relative ease in which bulk-foam experiments can be conducted. However, correlations observed in absence of oil do not always hold in presence of oil (Jones et al., 2016b). Here we plot the apparent viscosity of 70%-quality foam in porous medium as a function of the initial bulk foam volume (Figure 3.4-a) and foam half-life (Figure 3.4-b). These figures show there is a correlation between the apparent viscosity and bulk-foam behaviour, though with a large scatter in the trend. We also investigate the relation between the apparent viscosity in porous media and the product of initial bulk-foam volume and bulk foam half-life (Figure 3.4-c) which was introduced as the *Foam Composite Index* by Pu et al. (2017). The product

of initial bulk-foam volume and bulk foam half-life was introduced as the *Foam Composite Index* (FCI) by Pu et al. (2017) to describe bulk foam in presence of different crude oils.

The FCI of AOS foam and these oils could have been used to benchmark the apparent viscosity of the foams in presence of these oils in porous media. We observe a good correlation in in Figure 3.4-c and a smaller scatter in the trend than in Figure 3.4-a and Figure 3.4-b. This is in line with previous observations for foam in absence of oil; Chevallier et al. (2019) used an approach similar to the FCI to correlate bulk foam behaviour to foam behaviour in porous media. One implication is that if either the half-life or initial volume of bulk foam is poor, the foam performs poorly in the porous medium. Further research is needed to evaluate this correlation for different OCs, foams and porous media with different wettability.

Solely based on the GC analysis, TAN and TBN of a crude oil, it is not clear how a mixture of those components impact foam, in bulk or in porous media. Similarly, Pu et al. (2017) and Vikingstad et al. (2005) find there is no obvious way to predict the impact of a crude oil on foam based on its saturate, aromatic, resin and asphaltene (SARA) fractions. This suggests that, even for a relatively simple mixture of three pure OCs, for which we know the impact of the pure OCs on bulk foam, there is no obvious way to predict the impact of a mixture of those OCs on the foam. Thus, even if one knows the concentration of all the thousands of different components in a crude oil (Speight, 2014), and how these components impact foam separately, there is no obvious way to fully predict the impact of that crude oil on foam.

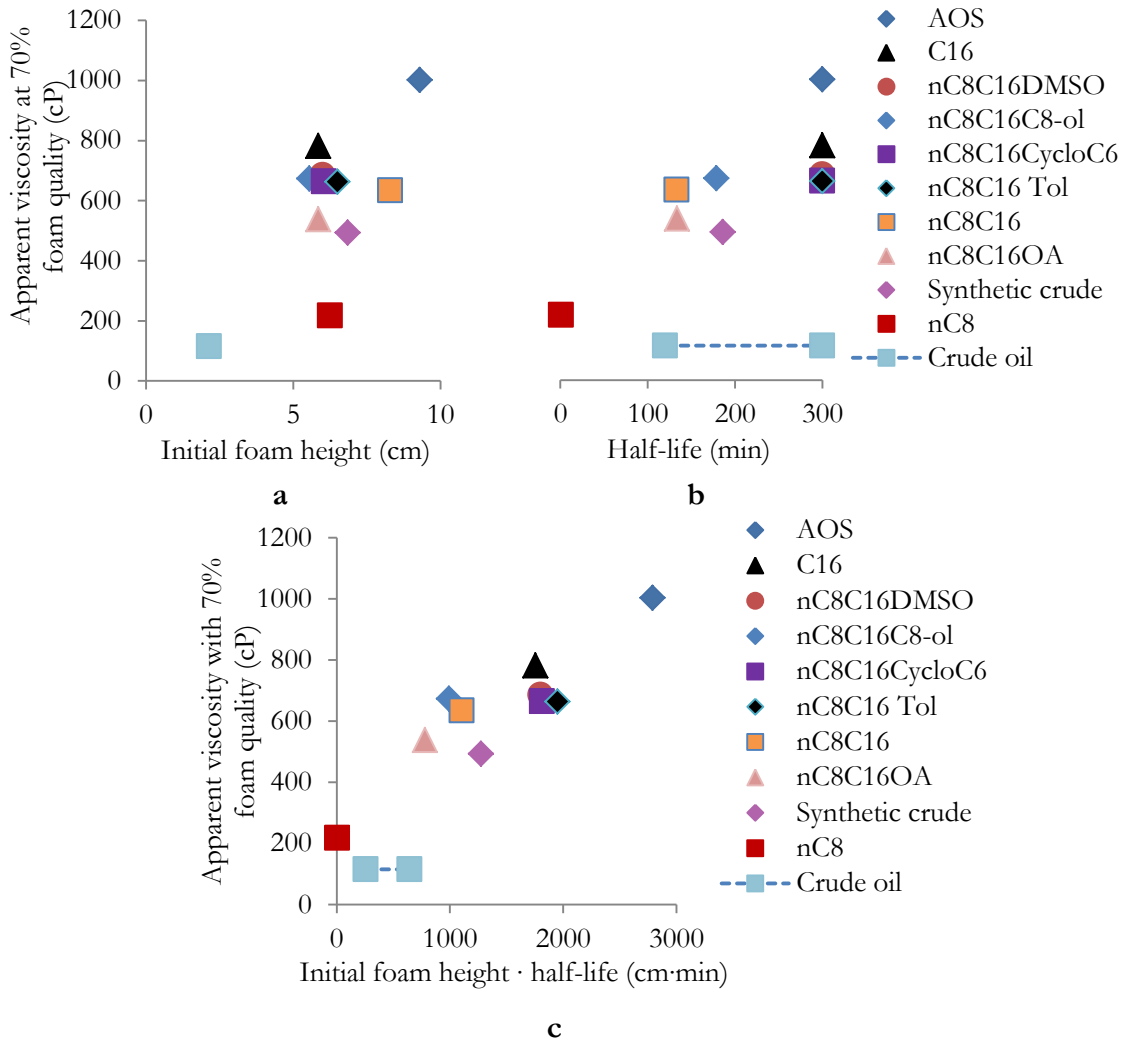

Figure 3.4: Top left: Apparent viscosity of 70%-quality foam in a porous medium with different OC mixtures, graphed as a function of initial bulk foam height (cm). Top right: Apparent viscosity of 70%-quality foam in a porous medium with different OC mixtures, graphed as a function of bulk foam half-life (min). Half-life values greater than 300 min are plotted as 300 min. The half-life of determination with crude oil was discontinued after 120 min. Bottom: Apparent viscosity of 70%-quality foam in a porous medium with the different OCs, graphed as a function of the product of initial bulk foam height (cm) and bulk foam half-life (min).

3.4. Conclusions

We mix several pure organic compounds (OC) to create a "synthetic" crude oil, with its composition based on the gas-chromatography analysis of the crude oil, and its total acid number and total base number. The pure OCs represent the following chemical species in the crude oil: light and heavy alkanes, aromatics, cycloalkanes, organosulfur compounds, organic acid and organic base. The impact of the pure OCs and the "synthetic" crude oil on foam (in bulk and in porous media) is compared to the impact of the crude oil. Compared to foam without OC, the crude oil results in approximately 80% lower apparent viscosity in a porous medium, and 80% smaller initial foam volume in bulk.

For foam in presence of different oils we find a good correlation between the foam apparent viscosity in a porous medium and the product of the bulk foam initial volume and half-life. Further research is needed to evaluate this correlation and its predictive power for different

OCs, foams, and porous media with different wettability. If this correlation holds for other OCs, foams, and porous media this correlation can be used as part of the screening procedure for foam application for EOR purposes.

We conclude that the effect of this crude oil on foam cannot be modelled by our synthetic crude oil. The impact of our synthetic crude oil is significantly less detrimental to foam than the actual crude oil, both in bulk and in a porous medium. The impact of our synthetic crude oil is almost the same as our mixture of n-octane, hexadecane and oleic acid. The other OCs added to our alkane mixture barely influenced the impact of our synthetic crude oil on foam, both in bulk and in a porous medium.

Furthermore, we conclude that it is not obvious how to correctly predict the impact of the OC mixture on a foam based on a complete composition of an OC mixture. This holds even if the impacts of all its components, separately, on foam are known. The impact of an OC mixture on foam is not necessarily the weighted average of the impact of the pure components, nor is its impact on foam necessarily skewed towards the impact of the most harmful component.

To our knowledge, the impact of crude oil on foam in porous media has not been reproduced with a synthetic oil mixture. We suggest that, screening of crude oil for foam application should be conducted with the crude oil itself and not a synthetic crude oil. If our tests were successful, our results could have been used to screen crude oils for foam application. However, before a field-application, experiments would have to be conducted with the actual crude oil.

4. The Impacts of Solubilized and Dispersed Crude Oil on Foam in a Porous Medium

The content in this chapter is submitted to a journal for publishing: Hussain, A. A. A., Vincent-Bonnieu, S., Kamarul Bahrim, R.Z., and Rossen, W.R. The impacts of solubilized and dispersed crude oil on foam in a porous medium.

4.1. Introduction

Gas can be injected into an oil field as an Enhanced Oil Recovery (EOR) process. However, gas suffers from poor sweep efficiency. Foam EOR can be used to reduce gas mobility, and partially compensate for the effect of permeability heterogeneity (Kapetas et al., 2015b; Moradi-Araghi et al., 1997). Phase mobility quantifies the ease with which the phase flows through the porous medium: it is defined as the ratio of the phase relative-permeability to the phase viscosity.

For field application, foam must be able to withstand the presence of crude oil to some degree. If foam is generated near the well in a region of low oil saturation, it still might not propagate to the production well. Thus the feasibility of foam generation far from an injection well is an important issue. With the distance between the injection well and production well usually more than 1200 ft. (366 m) (Texas Administrative Code, n.d.), and an interstitial velocity of 2 ft./day (0.6 m/day), the injected surfactant equilibrates with the crude oil in the reservoir for more than 600 days. This leads to the question whether foam can be created in situ if the surfactant has equilibrated with the crude oil (i.e. has solubilized crude-oil components).

In porous media, foam without oil shows two flow regimes: a high-quality regime, which reflects foam instability at a limiting water saturation or capillary pressure, and a low-quality regime, with strong shear-thinning behaviour as a function of gas superficial velocity (Alvarez et al., 2001). We define the foam quality as the gas fraction of the combined water and gas superficial velocities. There are various ways to characterize foam stability in the presence of oil, including column tests with "bulk" foam and core-flood tests, often with foam displacing an initial resident oil saturation, such as conducted by Simjoo et al. (2013). Jones et al. (2016b) and Meling and Hanssen (1990) relate foam behaviour in column tests to foam in porous media. They find a strong correlation between column and core-flood experiments conducted in the absence of oil, but poor correlation with the experiments in presence of oil.

The impact of different pure oils, in dispersed and solubilized form, on foam has been investigated by various researchers. Bergeron et al. (1993) conducted foam core-flooding experiments with foam without oil, pre-equilibrated with an alkane (dodecane), and pre-equilibrated with an aromatic (tetralin). They find that foam with solubilized dodecane achieves a lower pressure gradient, and foam with a solubilized aromatic tetralin achieves a higher pressure gradient, compared to -foam without oil. These experiments indicate that different solubilized oils can impact foam in different ways. Meling and Hanssen (1990) speculate that the impact of n-alkanes (n-octane, n-dodecane and n-hexadecane), dispersed as a separate phase, on foam in bulk and in porous media can be predicted by the impact of solubilized molecules on the interfacial properties between the gas and water phases. Lobo et al. (1989) report that bulk foam is destabilized by solubilized and dispersed dodecane and octane. Similarly, Lee et al. (2013) see the same impact of n-dodecane on foam when introduced as a dispersed phase and solubilized in the aqueous phase. From this they deduce that the observed impact of n-dodecane on bulk foam is solely caused by solubilized n-dodecane. However, when conducting the same experiments

with an aromatic hydrocarbon (toluene), they report foam destabilisation occurs with toluene in dispersed form and not in solubilized form, similar to what was observed by Vikingstad et al. (2005) with bulk foam. These findings indicate that the weakening of foam by a dispersed phase of short-chained alkanes can be attributed in part to solubilized oil molecules. In contrast they find that aromatic hydrocarbons weaken foam only in dispersed form and have no impact on, or can even strengthen, foam when in solubilized form.

In this chapter, we investigate the impact of a crude oil on foam, comparing solubilized oil and a dispersed oil phase, and determine the impact of the crude oil that can be attributed to solubilized components. To investigate the impact of solubilized crude oil, we conduct core-flood experiments with surfactant solutions pre-equilibrated with oil, where we co-inject gas and surfactant at different ratios but fixed total interstitial velocity: i.e., a foam-quality-scan. To gain a better understanding of which components within the crude oil impact the foam in porous media, we also conduct experiments with the surfactant solutions pre-equilibrated with hexane, to understand the impact of solubilized short alkanes from the crude oil. Furthermore, we conduct steady-state co-injection experiments with crude oil, gas, and water (with and without surfactant) to investigate the impact of crude oil as a separate phase on foam. To gain an understanding of how relative permeability, emulsification, and foam impact the total mobility with three-phase co-injection, we model our experiments using a simplified representation of the separate effects of three-phase flow, emulsification and foam.

4.2. Materials and procedures

The core used in our experiments is a Bentheimer sandstone, which has been described in previous work (Peksa et al., 2015). The porosity is 0.248 ± 0.019 and the measured permeability, k, of the core is 2.6 ± 0.2 × 10^{-12} m^2. The core length is 17 cm, with a diameter of 1 cm, mounted vertically. The cores are coated in epoxy resin, which results in an effective core diameter of 0.94 cm, and are mounted in aluminium core-holders, as done by Jones et al. (2016a and 2016b). The experiments were conducted at a temperature of 30°C and a back-pressure of 20 bars. The three fluids were injected from the bottom of the core, through relatively narrow tubes and connections, with an inner diameter of 0.75 mm, in order to minimise the droplet size of the entering phases.

Gas was injected into the core is nitrogen with a purity of 99.98%, supplied from a 200-bar gas cylinder. Synthetic seawater solution was used for the brine; see Table 4.1 for the composition. The crude oil used has a viscosity of 2.8 ± 0.03 cP and a density of 0.84 ± 0.01 g/cm^3, measured at 20°C. The anionic surfactant, C_{14-16} alpha olefin sulfonate (Witconate, supplied by AkzoNobel), was used as received and was set to 0.5 wt.% in all the surfactant solutions. The critical micelle concentration is roughly 0.003 wt.% at 23°C (Jones et al., 2016a). In the simplified modelling described below, we assume the viscosity of the surfactant solution to be roughly equal to that of the seawater solution, 0.85 ± 0.01 cP at 30°C (Sharqawy et al., 2010). To satisfy adsorption, the core as flooded with more than 10 pore volumes of surfactant solution before starting the foam-quality-scan experiments.

Table 4.1: Synthetic seawater composition.

Salts	Grams / litre
NaCl	**25.4**
KCl	**0.673**
$MgCl_2.6H2O$	**10.2**
$CaCl_2.2H20$	**1.47**
Na_2SO_4	**3.83**

Lee et al. (2013) find that solubilized n-dodecane can have a stronger detrimental impact on bulk foam (formed with sodium dodecyl sulfate) than the aromatic hydrocarbon toluene. Therefore we chose to conduct our core-flood experiment with a solubilized alkane. We conducted our experiments with hexane (supplied by VWR), because shorter alkanes in the oleic phase cause faster bulk foam collapse with AOS, and hexane in the oleic phase can increase AOS foam mobility in Bentheimer sandstone by almost a factor two (Tang et al., 2018b). Moreover, the process of oil solubilisation into micelles and resulting swollen micelles is most prominent with shorter alkanes (Langevin, 1992).

In some of our experiments surfactant solutions were equilibrated first with the crude oil or with hexane. Surfactant solution and crude oil were mixed as follows: 1029.1 +/- 0.1 grams of surfactant solution with 198.9 +/- 0.1 grams of crude oil in a 2-litre bottle, stirred daily for 11 days. With the hexane solution, 730.8 +/- 0.1 grams of surfactant solution were mixed with 80.7 +/- 0.1 grams of hexane for 10 days. The two-phase co-injection core-floods with pre-equilibrated surfactant were conducted in the same way as the foam-quality-scan core-floods.

The surfactant solution equilibrated with crude oil was first separated from the crude oil and any separate emulsion layer, then centrifuged at 2000 rpm for 2 hours, and finally filtered through a filter paper (Sartorius) with a pore size of 0.45 μm, under a pressure gradient imposed by a vacuum pump. As shown in Figure 4.1, all particles in the unfiltered solution have a size smaller than 0.45 μm, and thus we decided not to filter and centrifuge the solution equilibrated with hexane.

The surfactant (which is a mixture of $C_{14}H_{27}O_3S^-Na^+$ and $C_{16}H_{231}O_3S^-Na^+$) has a molecular length of about 2.3 nm, assuming carbon-carbon and carbon-sulphur bond-lengths of 1.5 Å and 1.8 Å respectively (Lide, 2015). This corresponds to a minimum micelle diameter of 4.6 nm. Applying Dynamic Light Scattering (DLS, by Malvern Zetasizer), we determined the micelle-size distribution of the surfactant solution equilibrated with crude oil, and surfactant solution without oil; see Figure 4.1. As also reported by Lee et al. (2014), the mode of the micelle-size distribution of the surfactant solution increases after equilibration with oil. However, unlike their case, the polydispersity (Malvern Instruments, 2004) of the micellar aggregates slightly decreases.

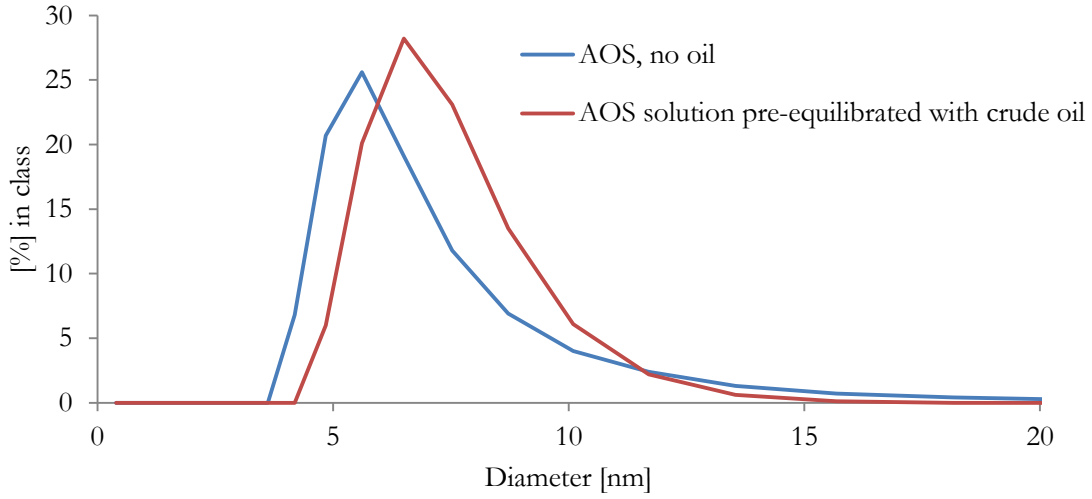

Figure 4.1: Size distribution of surfactant micelles, measured with the Malvern Zetasizer.

The surfactant concentration in the surfactant solution equilibrated with crude oil was determined by titration to be 0.37 +/- 0.01 wt.%; see Table 4.2. From Total Oil Content (TOC) measurements (using a Shimadzu TOC analyser and a Skalar Primacs^{SLC} TOC analyser), we deduce that the solubilized crude-oil content is 0.14 +/- 0.03 wt.%. We assume that the surfactant concentration of the pre-equilibrated solution decreases from 0.5 to 0.37 wt.% because of surfactant losses to the crude oil. We did not observe an emulsion when equilibrating the surfactant solution with hexane. We discuss the effect of the loss of this surfactant below.

Table 4.2: The measured and calculated surfactant and oil content of the surfactant solutions.

Description	Total carbon (ppm)	Oil content (wt.%)	Surfactant concentration (wt.%)
AOS solution without solubilized oil	**2880** ± 140 [a, b]	**-**	**0.50** ± 0.02 [a, b]
Solubilized crude oil in pre-equilibrated AOS solution	**3330** ± 140 [b]	**0.14** ± 0.02 [b, c]	**0.37** ± 0.01 [c]; surfactant concentration decreased by 0.13 wt.% due to depletion by emulsion, generated while equilibrating.
Solubilized hexane in AOS solution	**27×10^2** ± 2×10^2 [d]	Total oil + surfactant concentration: **0.44 – 0.51**	

[a] values calculated using the active content in the original AOS solution.

[b] values calculated from Shimadzu TOC analyser values.

[c] values calculated from the surfactant titration measurement. [d] values calculated with the Skalar Primacs^{SLC} TOC analyser values.

Interfacial-tension (IFT) values of less than 1 mN/m and 18 ± 1 mN/m were measured for crude oil with surfactant solution in synthetic seawater and for crude oil with synthetic seawater, respectively. These measurements were conducted using the Du Noüy–Padday method at room temperature (21 ± 1°C) and ambient pressure. Table 4.3 gives the surface tensions of the crude oil and the aqueous solutions. Table 4.4 gives the relevant interfacial tensions for the crude oil and the aqueous solutions, and the respective entering-, spreading-, and bridging-coefficient values and lamella number (Schramm and Novosad, 1990). The measured interfacial tension between crude oil and surfactant solution was below the measuring range of the device (1 – 350 mN/m). In our calculation of the range of foam-stability-coefficient values we use interfacial tensions of 0 and 1 mN/m. We assume the interfacial tension between crude oil and pre-equilibrated surfactant solution to be equal to that of crude oil and surfactant solution.

Table 4.3: Surface-tension values measured at ambient conditions.

Surface tension (mN/m)	
Crude oil	**27** ± 1
Synthetic seawater	**73** ± 1
Synthetic seawater with 0.5 wt.% AOS C14-16	**28** ± 1

Table 4.4: Interfacial-tension values measured at ambient conditions, and the calculated entering, spreading and bridging coefficients, and lamella number.

	Interfacial tension (mN/m)	Entering coefficient	Spreading coefficient	Bridging coefficient	Lamella number
Crude oil / synthetic seawater	**18** ± 1	**64**	**28**	**4870**	**0.6**
Crude oil / synthetic seawater + 0.5 wt.% AOS C14-16	**<1**	**2-3**	**1-2**	**95-96**	**4-∞**

Core-flood experiments were conducted with a total injection rate of 0.1 ml/min, which is equivalent to 6.8 ft./day ($2.4 \cdot 10^{-5}$ m/s) superficial velocity. To minimize any impact of hysteresis while conducting the foam-quality scan, in collecting data we alternated between low and high foam qualities. We define the foam-quality as the gas fraction of the combined gas and water injection rate.

The three-phase co-injection experiments without surfactant were conducted after the three-phase co-injection experiment with surfactant. To remove the surfactant from the core, we flooded the core with 190 PV of synthetic seawater to remove the surfactant. We preferred not flooding the core with a solvent (such as alcohol), to avoid the possibility of a solvent altering the core properties or a residual concentration of solvent later impacting oil-water interactions.

4.3. Results and discussions

We examine three different ways that the crude oil can impact pressure gradient compared to co-injection of gas and surfactant without oil: 1) oil weakening foam when solubilized, 2) oil as a separate phase impacting the three-phase relative permeabilities of water and gas, and 3) oil weakening the foam as a separate phase, possibly as an emulsion. We analyse our data to distinguish these three effects. Our analysis of the core-flood experiments is focused on the measured absolute-pressure data, from which we calculate the pressure gradient, ∇P [Pa/m]. Using the pressure gradient, we calculate the apparent viscosity of foam, μ_{app} [Pa·s], as follows:

$$\mu_{app} = \frac{k}{q} |\nabla P| \qquad \text{Eq. 4.1}$$

where q is the total superficial velocity [m/s] and k is the permeability of the porous medium [m^2]. Eq. 4.1 gives apparent viscosity [Pa·s]; below we report results in cP (1000 times the value in Pa·s). A benchmark core-flood experiment is conducted without any oil. This produces a relatively strong foam, similar to that reported by Jones et al. (2016a), who conducted core-flood experiments with the same surfactant and porous medium at similar salinity. The apparent viscosity is presented as a function of the gas fractional flow (foam-quality) in Figure 4.2. The shape of the curve at foam qualities between 60% and 95% is similar to what was observed by Jones et al. (2016a) with the same surfactant (Figure 4.3).

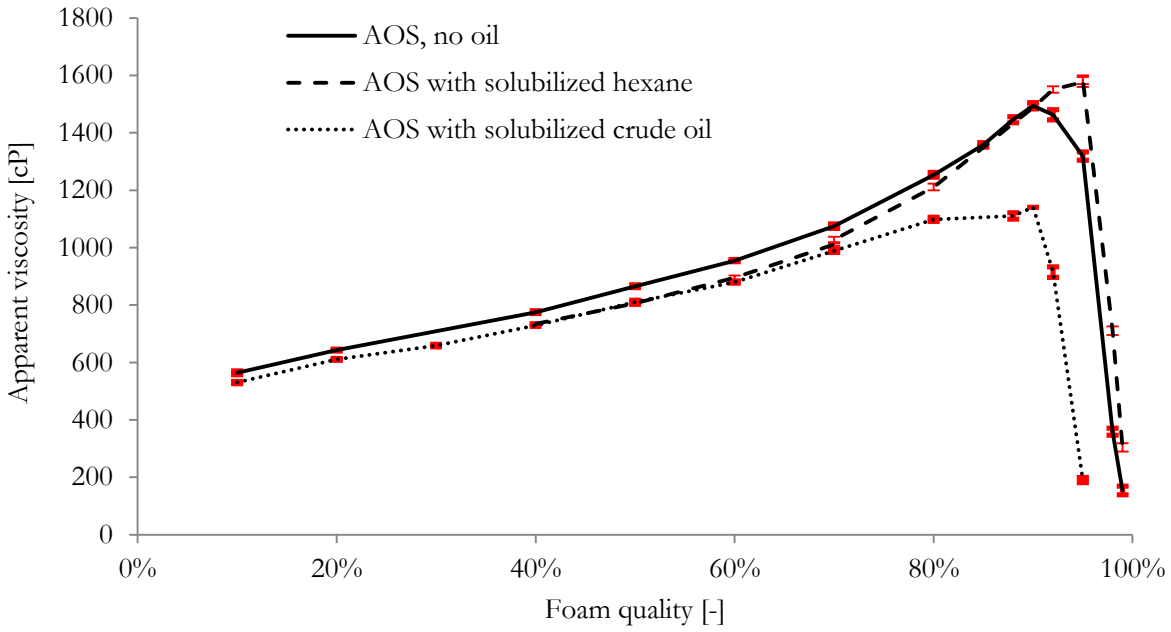

Figure 4.2: Foam apparent viscosity as a function of foam quality for foams made without solubilized oil, and with surfactant with solubilized crude oil and with solubilized hexane. The lines are to guide the eye. Bars indicate standard deviation of measurements over time in the given test.

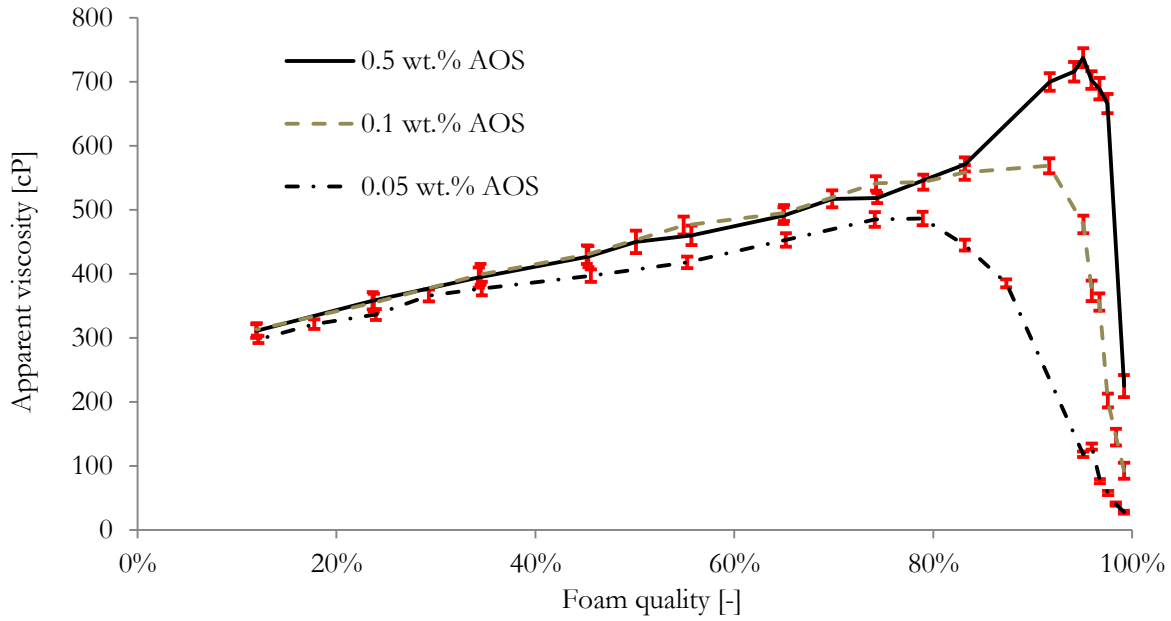

Figure 4.3: Foam apparent viscosity as a function of foam quality at various surfactant concentrations, from Jones et al. (2016a), with no oil present. The lines are to guide the eye. Bars indicate standard deviation of measurements over time in the given test.

4.3.1. Effect of solubilized oil on foam

In the foam scan with solubilized oil, the maximum apparent viscosity is about 1200 cP with solubilized crude oil and 1600 cP with solubilized hexane, indicating that foam is generated in both cases (Figure 4.2). Therefore, we conclude that solubilized oil, whether crude oil or hexane, does not prevent AOS-foam creation. However, the foam-scan results without oil and with solubilized crude oil differ in two aspects: foam in the high-quality regime is weaker, and the shear-thickening behaviour (concave-upward shape of the curve) in the low-quality regime is not

observed with solubilized crude oil. At foam qualities 40 – 60%, surfactant solution equilibrated with hexane shows an apparent-viscosity profile similar to surfactant solution equilibrated with crude oil, and is only 5 – 10% different from that without any oil. However, as foam quality increases, the apparent viscosities with solubilized hexane and without any oil are almost identical. The maximum apparent viscosity of foam made with surfactant solution equilibrated with crude oil is approximately 20% lower than with surfactant solution without solubilized oil. This is a reflection of weaker foam in the high-quality regime. However, the decrease of apparent viscosity may be caused in part by the decrease of surfactant concentration. The surfactant concentration in the solution with solubilized crude oil is 0.37 wt.%, whereas the surfactant concentration in the surfactant solution without oil is 0.5 wt.% (Table 4.2). Jones et al. (2016a) showed that foam apparent viscosity decreases by about the same fraction for surfactant concentration decreasing from 0.5 wt.% to 0.1 wt.%; see Figure 4.3.

Because, for the experiment with crude oil, both the surfactant concentration changed and some oil was solubilized (see Table 4.2), it is not clear how much the decrease in surfactant concentration and presence of solubilized oil separately impacted foam apparent viscosities. Nonetheless, it can be said that the observed behaviour of foam equilibrated with hexane cannot explain the major impact of hexane as a separate oleic phase on foam in porous media reported by Tang et al. (2018). The impact of solubilized oil on steady-state foam apparent viscosity is limited in our results and cannot explain the observed three-phase flow (crude oil, surfactant, gas) results described in the next section.

4.3.2. Effect of 3-phase relative-permeability

Three-phase flow without any foam or emulsion can result in high apparent viscosity, compared to water, due to three-phase relative-permeability effects. Three-phase co-injection experiments without surfactant (using Soltrol 170 as a model oil, composed of C12-C14 iso-alkanes, with a viscosity of 2 cP at 37.8°C) in Bentheimer sandstone produce apparent viscosities in the range of 100 cP simply through three-phase relative-permeability effects (Alizadeh and Piri, 2014).

In our analysis of the steady-state co-injection experiment with surfactant, gas, and 1% fractional flow of crude oil, we assume that the oil saturation is close to the gas-flood residual oil saturation. The results of the three-phase co-injection experiments, Figure 4.4, lack the characteristic two foam regimes seen in Figure 4.2. Furthermore, the magnitude of foam apparent viscosity with oil as a separate phase without surfactant is lower (maximum 180 cP, Figure 4.4) than with foam with solubilized oil (maximum 1500 cP, Figure 4.2). Oil fractional flow is also important: apparent viscosity increases with increasing oil fractional flow (and, by implication, increasing oil saturation). This result is somewhat counter-intuitive, since foam is expected to be weaker at higher oil saturation (Mannhardt and Svorstøl, 1999). However, the increase in apparent viscosity with increasing oil fractional flow in Figure 4.4 could be due in part to three-phase relative-permeability effects at greater fractional flow of oil.

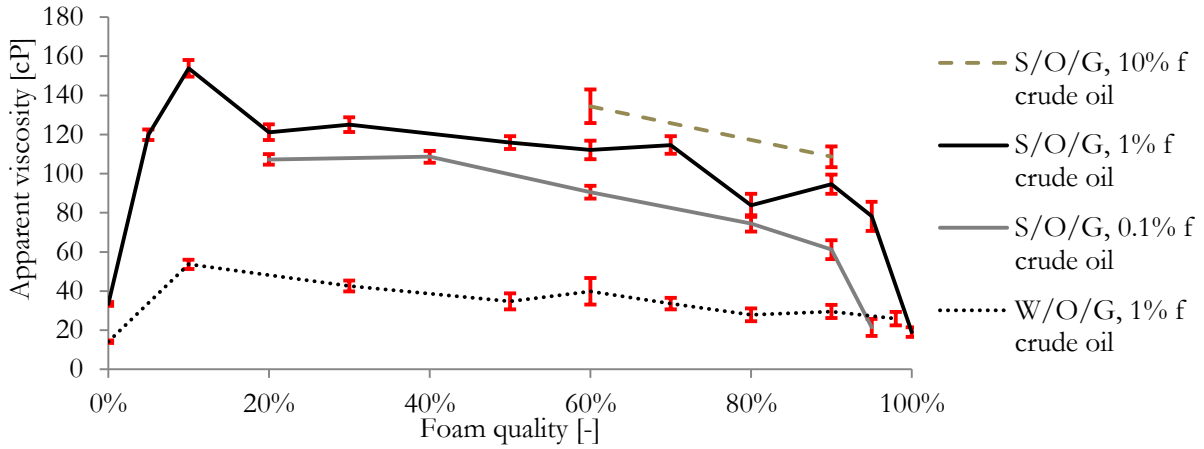

Figure 4.4: Foam apparent viscosity as a function of foam quality for three-phase co-injection experiments. The foam quality is defined as the gas fraction of the gas- and aqueous-phase volumetric injection rate. The line is to guide the eye. S is aqueous surfactant solution, W brine without surfactant, O oil and G gas. f is total volume % oil in the injected fluids. Bars indicate standard deviation of measurements over time in the given test.

4.3.3. Effect of emulsification and weaker foam

We observed an emulsion and fast-collapsing foam after shaking a test tube with crude oil and seawater (without surfactant). With surfactant we observed a finer emulsion, and finer-textured foam. We believe that these qualitative observations correspond to the phase interactions in the core. In Figure 4.4 the apparent-viscosity curves as a function of foam quality have a similar shape, but differ in magnitude. The higher apparent viscosity at lower foam qualities, compared to the trend without oil, indicate that the aqueous phase has a reduced mobility. Moreover, in our three-phase co-injection experiments (with and without surfactant) we observe an emulsion in the effluent. Therefore, the higher apparent viscosity observed with 1% oil fractional flow with surfactant in the aqueous phase, compared to that without surfactant, is likely to reflect, at least in part, a more-viscous emulsion generated with surfactant than without.

Similarly, the higher apparent viscosity at higher foam qualities, as observed with foam without oil (see Figure 4.2), indicates that the gas phase has a reduced mobility, which indicates stronger foam compared to the case without surfactant.

Thus, we hypothesize that the relatively high apparent viscosities achieved with three-phase co-injection is a combined result of relative permeability, effects of emulsification, and weak foam. The relative-permeability effect reduces gas and water mobilities as oil fractional flow increases. Oil emulsification reduces oil mobility and weaker foam leads to increased gas mobility compared to foam without oil.

4.3.4. Modelling of laboratory experiments

There are three possible causes of reduced mobility in our experiments; relative permeability, effects of emulsification, and weak foam. To distinguish between them, we compare the data to a very simple model qualitatively incorporating the three effects. We chose to use a simple model with three fitting parameters because fewer fitting parameters means there are fewer solutions, allowing one to make firmer conclusions on which parameters impact the observed behaviour. We model our laboratory experiments with three-phase relative-permeability curves and viscosity-multiplication factors for the different phases. We use the three-phase

relative-permeability data of Alizadeh and Piri (2014) and a Corey-style relative-permeability relationship as in Eq. 4.2. In this relationship, n_α is the Corey exponent, $S_{r,\alpha}$ the residual saturation, and $k^o_{r,\alpha}$ is the end-point relative-permeability of phase α. See Table 4.5 for our Corey parameter values, based on a fit to the data of Alizadeh and Piri (2014). Thus we assume that the residual saturations in our case are equal to those measured without surfactant in the aqueous phase and with a model oil. Moreover, we foam-flooded the core before conducting the three-phase co-injection experiments, therefore we assume there is trapped gas in the porous medium, even when gas fraction-flow is zero. The water, oil, and gas relative-permeability fits to the experimental data are shown in Figure A1-a, b, and c in Appendix A.

$$k_{r,\alpha} = k^o_{r,\alpha} \times \left(\frac{S_\alpha - s_{r,\alpha}}{1 - s_{r,o} - s_{r,g} - s_{r,w}} \right)^{n_\alpha} \qquad \text{Eq. 4.2}$$

Table 4.5: Corey-parameter values for the relative-permeability functions for each phase.

	Water	Oil	Gas
n_α	3.5	4	3.8
$s_{r,\alpha}$	0.089	0.108	0.24
$k^o_{r,\alpha}$	0.1	0.35	0.6

Figure 4.5 shows three model fits, each with only the water, gas, or oil viscosity increased (increased by 8×, 300× and 100×, respectively). These figures indicate that the apparent-viscosity trend as a function of foam quality cannot be modelled with an increased gas viscosity only, as is usually done when modelling foam in the presence or absence of oil (Farajzadeh et al., 2012). Reducing water mobility alone misses the high-quality data and has a negative R^2 because the sum of the discrepancy between the data and the curve is larger than the sum of the discrepancy between the data and a horizontal line equal to the average of the data. A model for reduced gas mobility with foam misses the data at low foam quality. Increasing oil viscosity alone does a somewhat better job, but it is hard to identify a mechanism for reducing oil mobility by such a large factor and without affecting gas or water mobility. Moreover, after shaking a test tube with crude oil and surfactant solution we observed foam and an emulsion. This indicates that modelling three-phase co-injection by increasing only the oil or gas viscosity contradicts our simple test tube experiment.

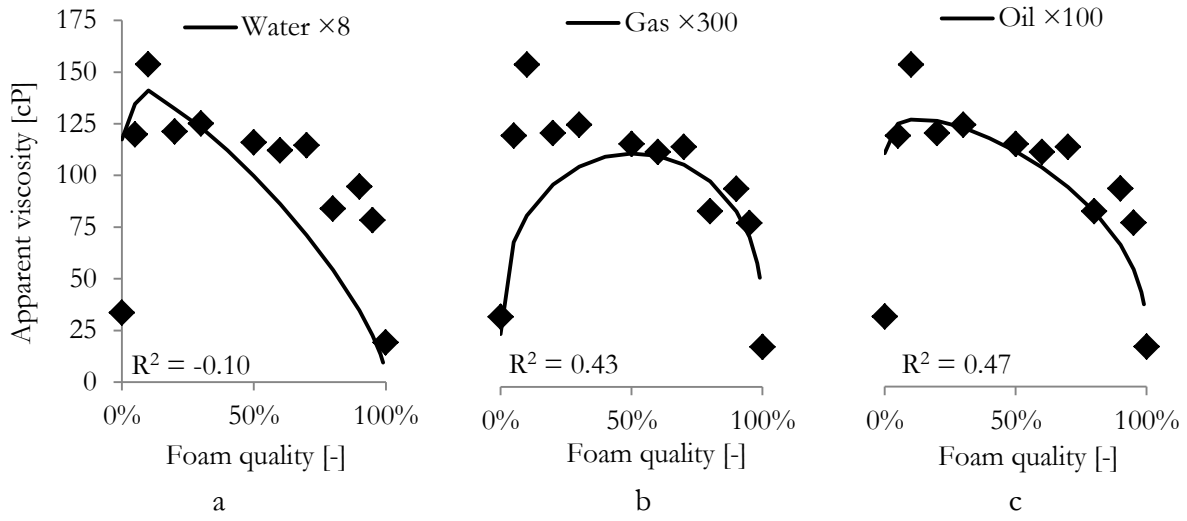

Figure 4.5: The apparent viscosities achieved at different foam qualities in the three-phase co-injection experiments, with surfactant in the aqueous phase and 1% crude oil fractional flow. Figure a, b, c, show the modelled apparent viscosity vs foam quality with an increased water (×8), gas (×300), or oil (×100) viscosity, respectively.

Figure 4.6-a shows the model fits with a single viscosity multiplier for all the three-phases (4.5×); Figure 4.6-b with only the water and gas viscosities increased (by 3× and 90×, respectively); and Figure 4.6-c with only the oil and gas viscosities increased (by 13× and 90×, respectively). These figures illustrate that no adjustment to a single phase mobility fits the data. More-complex, even mechanistic, foam models still could not improve the fit in Fig. 5-b by adjusting gas mobility alone, since the biggest deviation is at low foam quality. Thus, we believe this experiment should be modelled by increasing both gas and either water or oil viscosity (Figure 4.6-c).

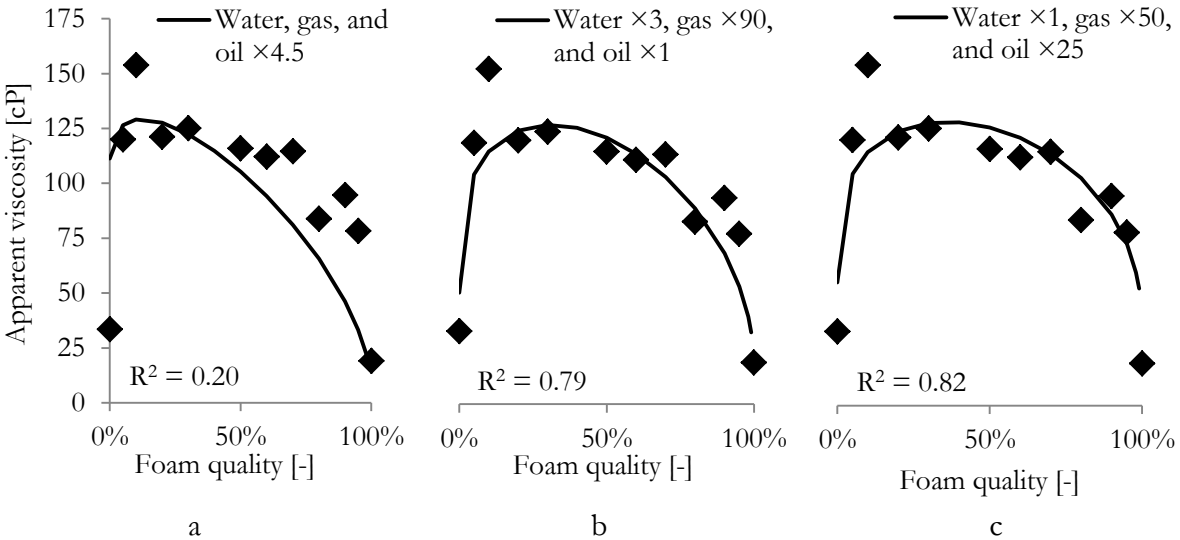

Figure 4.6: The apparent viscosities achieved in the three-phase co-injection experiments with surfactant, gas and 1% oil fractional flow, modelled with three sets of apparent phase-viscosity multipliers.

Figure B1-a in Appendix B shows the model fit for the three-phase co-injection data with 1% oil fractional flow and without any surfactant in the aqueous phase. Figure B1-b shows the model fit for the three-phase co-injection data with 0.1% oil fractional flow with surfactant in the

aqueous phase. These figures illustrate that the proposed model can capture our observed three-phase flow behaviour with different fractional flows, with and without surfactant. However, further work needs to be conducted to assess the sensitivity of the viscosity multipliers to the oil and water fractional flows. Our results show that complete and predictive flow modelling for this foam-oil combination requires a more-detailed model for both foam and emulsification. Specifically, Figure 4.6-b and c show that to model three-phase flow with such an oil, an increased oil viscosity or increased water viscosity needs to be included in the model to account for emulsification.

4.4. Conclusions

Solubilized crude-oil experiments (pre-equilibrating our surfactant solution with crude oil or hexane) show that the impact of our solubilized crude oil on AOS foam is limited, and does not explain the behaviour we observe with three-phase co-injection. We do not observe significant impact of solubilized hexane on AOS foam in porous media, indicating that the large impact of dispersed hexane on AOS foam (Tang et al., 2018b) cannot be accounted for by solubilized hexane.

Experiments with crude oil co-injected with gas and water show that co-injection of crude oil, gas, and water (with and without surfactant) resulted in similar trends in apparent viscosity as a function of foam-quality. With our simplified model, the apparent viscosities in three-phase-flow cannot be modelled with reduced gas mobility only; it requires reduced liquid (either water or oil) mobility as well. Furthermore, the apparent viscosity increases with increasing oil fractional flow (from 0.1% to 10%), which could be explained by the three-phase relative-permeability effects and emulsions generation in the core. Lastly, we did not observe foam in the effluent, though we did observe fast-collapsing foam when shaking a test-tube with crude oil and water (with and without surfactant).

5. Impact of crude oil on pre-generated foam in porous media

The content in this chapter is submitted to a journal for publishing: Hussain, A. A. A., Vincent-Bonnieu, S., Kamarul Bahrim, R.Z., Pilus, R. M. and Rossen, W.R., Impact of crude oil on pre-generated foam in porous media.

5.1. Introduction

Most research on the impact of (crude) oil on foam in porous media is conducted applying one of the following four methods:

- Injection of pre-generated foam injection into a core pre-saturated with oil (Aarra and Skauge, 1994; Kristiansen and Holt, 1992; Tang, 2019)
- Co-injection of oil, gas, and surfactant into a core (Tang et al., 2018b)
- Injection of surfactant and gas into a core (partly) pre-saturated with oil (Raza, 1970; Simjoo, 2012)
- Injection of pre-generated foam into a microfluidics chip, where oil is injected some distance downstream from the main inlet (Schramm et al., 1993; Schramm and Novosad, 1990)

However, these processes do not necessarily represent what happens with the application of foam for enhanced oil recovery (EOR), where foam can sometimes be generated in the absence of oil near the well. This (pre-)generated foam then propagates into regions richer in oil, where the different phases interact. A difference in flow characteristics between co-injection of three separate phases and co-injection pre-generated foam and oil arises from the difference in how oil impacts foam, i.e. by anti-foaming and/or de-foaming. Anti-foamers inhibit foam formation, and de-foamers destabilize an existing foam. For bulk foams outside porous media, de-foamers usually act on the outer surface of the foam (Pugh, 1996). By co-injecting gas, surfactant solution and oil, it is possible that foam is not created, due to strong anti-foaming impact by the oil. Tang (2019) reports completely different behaviour when injecting pre-generated foam than when co-injecting surfactant solution and gas into a core at waterflood-residual oil saturation. This indicates that, as with bulk foam, the impact of oil on pre-generated foam can be different from its impact on foam generation. By injecting foam pre-generated outside the porous medium, there is an uncertainty whether the characteristics of the injected foam are the same as in-situ-generated foam, especially if the foam generator has different properties than the core (Falls et al., 1989). This approach is also complicated by the capillary end effect at the outlet face of the first porous medium and coarsening of foam during transport to the second. Co-injecting both oil and pre-generated foam at the core inlet can result in oil weakening the foam at the T-junction of the apparatus tubing or in the injection plate. Therefore, we choose to investigate the impact of crude oil on foam by co-injecting surfactant solution and gas from the face of the core, and oil some distance downstream from the coreface, to investigate the impact of crude oil on in-situ pre-generated foam. This is similar in intent to the experiments conducted by Schramm and Novosad (1990) in glass micromodels. For foams that are weakened by oil, they report that the foam lamellae transported oil droplets for some distance before rupturing, after which the following lamellae picked up and transported the oil droplets.

In the next section of this chapter we present an overview of the materials we use for our experiments and experimental procedures. Using a relatively narrow core allows rapid contact between injected oil and foam, in a realistic porous medium much larger than pore dimensions.

That section is followed by an overview and discussion of our experimental findings and then our conclusions.

5.2. Materials and procedure

We used anionic surfactant $C_{14/16}$ Alpha Olefin Sulfonate (AOS, brand-name Witconate, supplied by AkzoNobel) and a proprietary mixture of anionic and amphoteric surfactants, referred to here as surfactant A. We prepared all the surfactant solutions with 0.5 wt.% surfactant concentration. Synthetic seawater solution was used for the brine; see Table 5.1 for its composition. For AOS the critical micelle concentration (CMC) is roughly 0.003 wt.% at 23°C (Jones et al., 2016a). To satisfy adsorption, the core was flooded with more than 10 pore volumes of surfactant solution before conducting experiments. Nitrogen gas is injected into the core with a purity of 99.98%, supplied from a 200-bar gas cylinder. The crude oil has a viscosity of 3.8 ± 0.03 cP and density of 0.84 ± 0.01 g/cm^3, measured at 20°C.

Table 5.1: Synthetic seawater composition

Salts	**Grams/ litre**
NaCl	**25.4**
KCl	**0.673**
$MgCl_2$.6H2O	**10.2**
$CaCl_2$.2H20	**1.47**
Na_2SO_4	**3.83**

For our experiments with AOS we used Bentheimer sandstone, which has a porosity of about 0.25 (Peksa et al., 2015). By water-flooding the core we determined the permeability, k, to be 2.6 ± 0.2 × 10^{-12} m^2. The experiments with surfactant A were conducted with Berea sandstone, which has a porosity of about 0.2 (Kapetas et al., 2015b; Øren and Bakke, 2003). By pumping water through a water-saturated core we determined the permeability to be 0.13 ± 0.005 × 10^{-12} m^2. The cores are 0.22 m in length and are 1 cm in diameter. The cores are coated in epoxy resin, which results in an effective core diameter of 0.94 cm, and are mounted in aluminium core-holders, as was done by Jones et al., (2016a, 2016b).

Nitrogen and surfactant solution were injected from the bottom coreface, reached through relatively narrow tubes and connections, with an inner diameter of 0.75 mm, to minimize the droplet size of the entering phases. Oil was injected 5.5 cm from the main inlet; see Figure 5.1. For the experiments with AOS at 50, 70 and 95% foam quality, the oil was injected with a single syringe pump from a single inject port; for all the other experiments with two syringe pumps from two different injection ports. The relatively narrow core allows rapid contact between the injected crude oil and pre-generated foam, especially when oil is injected from both sides. The experiments were conducted at a controlled temperature of 30°C with AOS, and at 90°C with surfactant A, and both with a back-pressure of 40 bar.

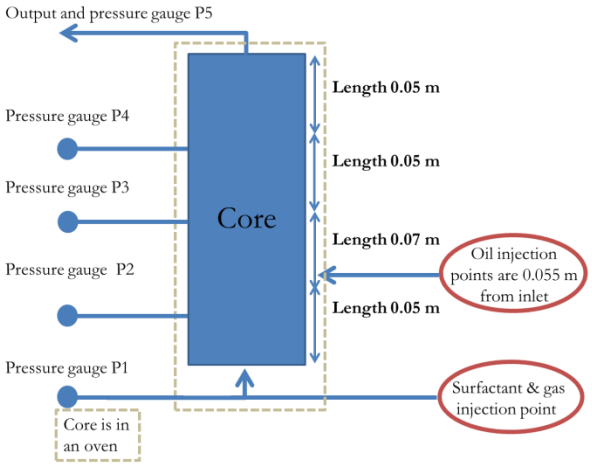

Figure 5.1: Schematic of the apparatus used for these experiments. Note that there are two oil-injection points 0.055 m from the main inlet on opposite sides of the core. (Only one is shown here to avoid clutter.)

Interfacial-tension values of <1 mN/m and 18 ± 1 mN/m were measured between crude oil and surfactant solution and synthetic seawater, respectively. These measurements were conducted using the Du Noüy–Padday method at room temperature (21 ± 1°C) and ambient pressure. Table 5.2 gives the surface tensions of the crude oil and the aqueous solutions. Table 5.3 gives the relevant interfacial tensions for the crude oil and the aqueous solutions, and the respective values of entering, spreading, and bridging coefficients and lamella number.

Table 5.2: Surface-tension values measured at ambient conditions.

Surface tension (mN/m)	
Crude oil	**27** ± 1
Synthetic seawater	**73** ± 1
Synthetic seawater with 0.5 wt.% AOS C14-16	**28** ± 1

Table 5.3: Interfacial-tension values measured at ambient conditions, and the calculated entering, spreading and bridging coefficients, and lamella number. The measured interfacial tension between crude oil and surfactant solution was below the measurement range of the device (1 – 350 mN/m). We assume an interfacial tension of 1 mN/m in our calculation of the foam-stability coefficients.

	Interfacial tension (mN/m)	Entering coefficient	Spreading coefficient	Bridging coefficient	Lamella number
Crude oil / synthetic seawater + 0.5 wt.% AOS C14-16	**<1**	**2**	**1-2**	**96**	**8**

We prepared our surfactant solution with solubilized oil as follows: we mixed AOS surfactant solution (1029.1 +/- 0.1 g) and crude oil (198.9 +/- 0.1 g) in a 2-litre bottle, and stir daily for 11 days. We then separated the surfactant solution from the crude oil and any separate emulsion layer by using a separation funnel. To remove any droplets from the surfactant solution, we centrifuge the solution at 2000 rpm for 2 hours, and finally filter through a filter paper (Sartorius) with a pore size of 0.45 μm, under a pressure gradient imposed by a vacuum pump. The surfactant concentration in the surfactant solution equilibrated with crude oil was

determined by titration to be 0.37 +/- 0.01 wt.%. From Total Oil Content (TOC) measurements (using a Shimadzu TOC analyser and a Skalar Primacs^{SLC} TOC analyser), we deduce that the solubilized crude oil content was 0.14 +/- 0.03 wt.%; see Table 5.4. We assume that the reduction in surfactant concentration by 0.13 wt.% detected by titration reflects surfactant consumption by emulsions or solubilisation into the oil when equilibrating the surfactant solution.

Table 5.4: The measured and calculated surfactant and oil content of the surfactant solutions used.

Description	Total carbon (ppm)	Oil content (wt.%)	Surfactant concentration (wt.%)
Initial AOS solution	**2878** ± 140 [a, b]	**-**	**0.50** ± 0.02 [a, b]
AOS solution with solubilized crude oil	**3329** ± 140 [b]	**0.14** ± 0.02 [b, c]	**0.37** ± 0.01 [c]; difference assumed due to surfactant lost to oil-water emulsion

[a] *values calculated with the active content in the initial AOS solution.*

[b] *values calculated with Shimadzu TOC analyser values.*

[c] *values calculated with the surfactant titration measurement.*

Core-flood experiments with both AOS and surfactant A were conducted with a total injection rate of 0.1 ml/min and 0.02 ml/min respectively, which is equivalent to superficial velocities of 6.8 ft/day and 2 ft/day. To minimize any impact of hysteresis while conducting the foam-quality scan, in collecting data we alternated between lower and higher foam qualities. We define foam quality as the gas fraction of the combined gas and water injection rate (i.e., excluding oil).

After we reached steady-state in an experiment, we started to prepare the core for the following experiment. To achieve an oil saturation greater than will be achieved with the subsequent experiment we stop gas injection but continue injection of surfactant solution at 0.001 ml/min to prevent oil moving upstream. We injected at least 3 ml of oil (at 0.05 ml/min), more than one pore volume of the three downstream sections. This experimental procedure allows us to investigate the steady-state behaviour of pre-generated foam in the presence of crude oil at various oil fractional flows and initial oil saturations.

5.3. Results and discussions

In each section of the core we calculate the "apparent viscosity" using the average pressure gradient over that section and assuming single-phase flow. We define the dimensionless apparent viscosity as the ratio of apparent viscosities observed with pre-generated foam in the presence of oil to the apparent viscosity observed in section 2 in the absence of oil.

5.3.1. AOS foam and crude oil

Figure 5.2-a and b show the dimensional and dimensionless apparent viscosities, respectively, as a function of position along the core, for different foam qualities with AOS surfactant. AOS foam progressively weakens after it comes into contact with crude oil. Higher-quality foams experience a steeper and greater decline in apparent viscosity over the length of the

core than lower-quality foams. The decline is most rapid with surfactant pre-equilibrated with the crude oil. However, apparent viscosity at the end of the core is similar for foam with pre-equilibrated surfactant (126 cP) and with surfactant which had not previously been in contact with oil (167 cP).

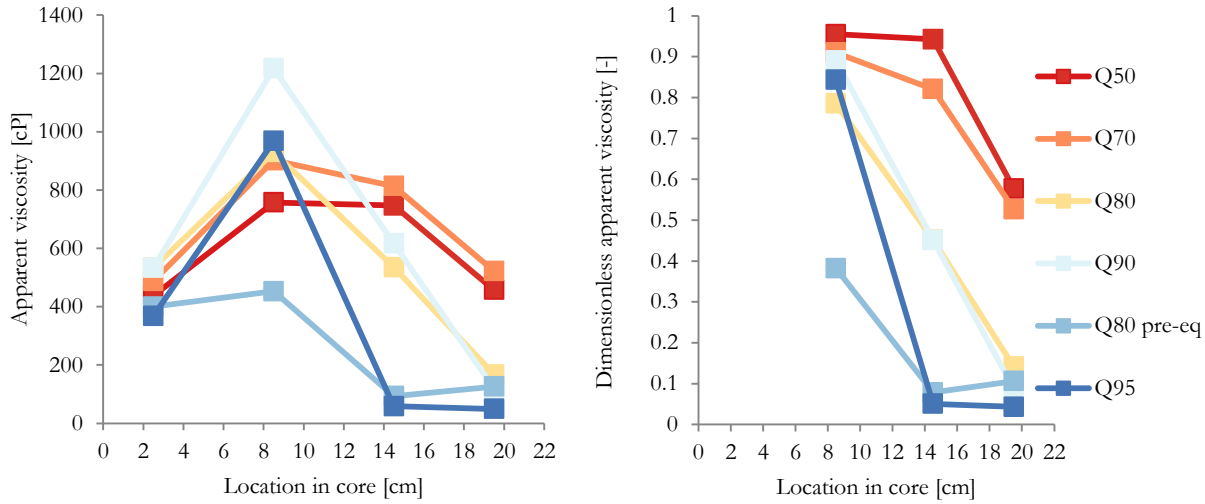

a b

Figure 5.2: Left: apparent viscosity [cP] over the length of the core for different foam qualities with AOS. Right: dimensionless apparent viscosity [-] over the length of the core for the same experiments. All experiments were conducted with 0.1% oil fractional-flow. Q50: 50% foam quality, etc. Pre-eq: surfactant solution pre-equilibrated with oil.

Figure 5.3 shows apparent viscosity as a function of foam quality in the different sections of the core. It also shows the apparent viscosity observed in three-phase co-injection experiments, where the oil, surfactant solution and gas are injected from the same port, with a total superficial velocity of 6.8 ft/day. Compared to the other reported experiments here, the three-phase co-injection experiments were conducted with the same materials and set-up, except with a shorter core (0.17 m vs. 0.22 m). The apparent viscosities in that case are calculated over a section starting 5.25 cm from the inlet to 5.25 cm from outlet of the core. As foam propagates through the core, the apparent viscosity gradually decreases. We believe that, in a sufficiently long core, apparent viscosities with pre-generated foam and oil would approach those with three-phase co-injection. It is unclear why apparent viscosity increases in the last section of the core with pre-equilibrated foam (Figure 5.2), as we did not observe this in any other experiments.

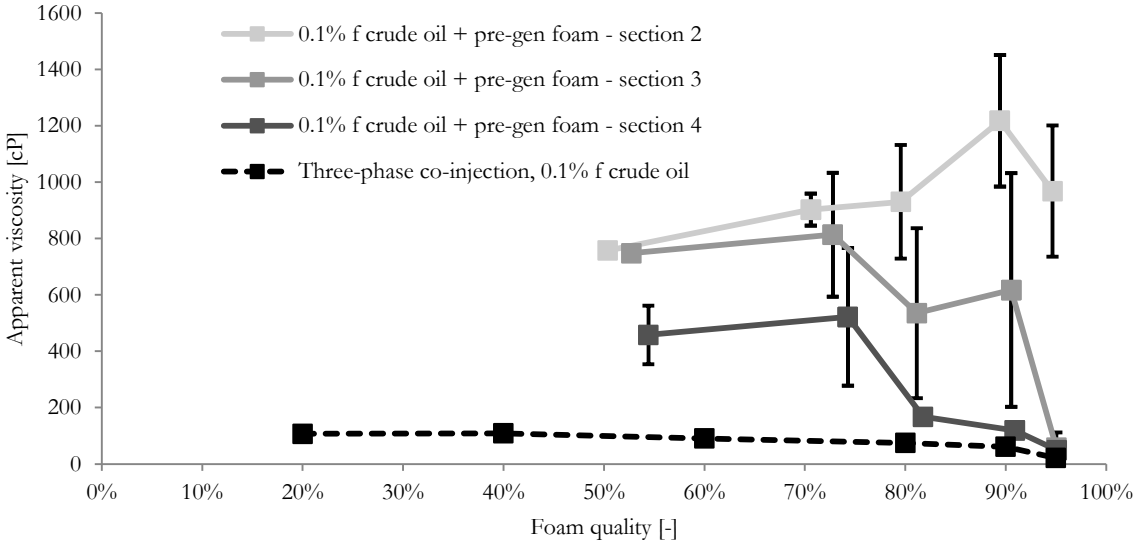

Figure 5.3: Apparent viscosity as a function of foam quality for pre-generated foam in contact with oil in different sections of the core, compared to three-phase co-injection. 0.1% f crude oil: 0.1% injected fractional flow of crude oil.

These results are consistent with the results of Schramm and Novosad (1990), who showed that foam lamellae in micromodels can travel some distance with oil droplets in them before rupturing. This indicates that pre-generated foam that comes into contact with oil in a porous medium does not necessarily collapse instantaneously, and can travel some distance on the core scale.

Aarra and Skauge (1994) and Kristiansen and Holt (1992) conducted similar experiments to these, where they pre-generated AOS-foam with qualities 65% - 95% outside their core and injected the foam into a core with crude oil at a residual saturation. As we do, they observed decreasing apparent viscosity along the length of the core for foam qualities between 65% and 95% in the presence of oil. Their results, together with ours, show that the impact of crude oil on pre-generated foam is a function not only of oil saturation and fractional flow, but also a function of foam quality.

5.3.2. Surfactant A foam and crude oil

Figure 5.4 and Figure 5.5 show the apparent viscosity of foam with surfactant A in the absence of oil and of pre-generated foam in the presence of oil, respectively, over the length of the core. Similar to the experiments with AOS, the apparent viscosity decreases progressively after the first contact of the pre-generated foam with the crude oil. However, unlike the experiments with AOS, an abrupt increase in apparent viscosity is observed as the pre-generated foam first contacts oil. Figure 5.4 and Figure 5.5 show that the apparent viscosity observed at first contact of oil and 40%-quality foam increases with an increasing fractional-flow of oil from 0 to 10%. We believe that the increase in apparent viscosity at first contact with oil reflects the combined effects of reduced relative permeabilities in three-phase flow and emulsion generation. Emulsion was observed in the core effluent in this experiment. After first contact, a steeper decrease in apparent viscosity occurs with 10% oil fractional flow than with 1%. This is consistent with observations in microfluidics by Schramm and Novosad (1990), who showed that

foam is weakened by oil droplets carried in the foam lamellae. Greater oil fractional flow means there is more oil in contact with the foam to destabilize it.

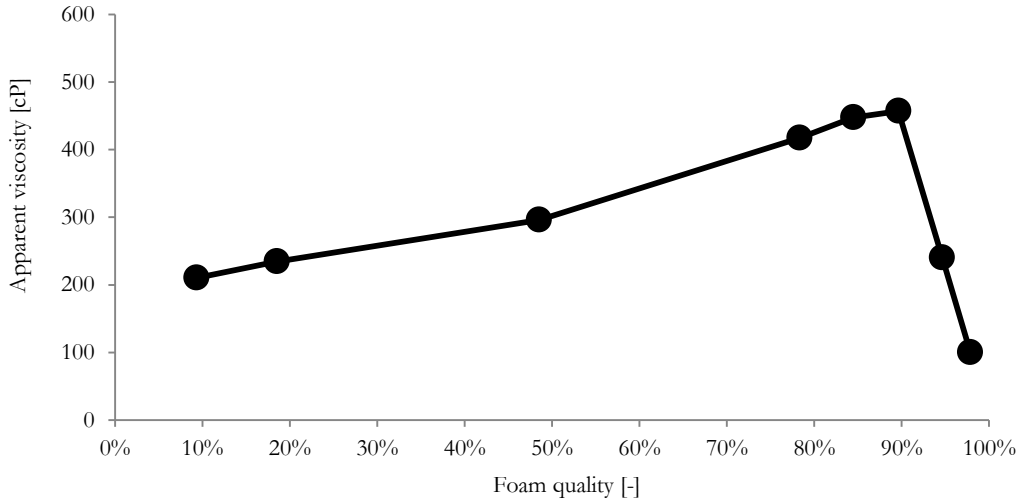

Figure 5.4: Surfactant-A foam apparent viscosity as a function of foam quality, in the absence of oil, in the third section of the core.

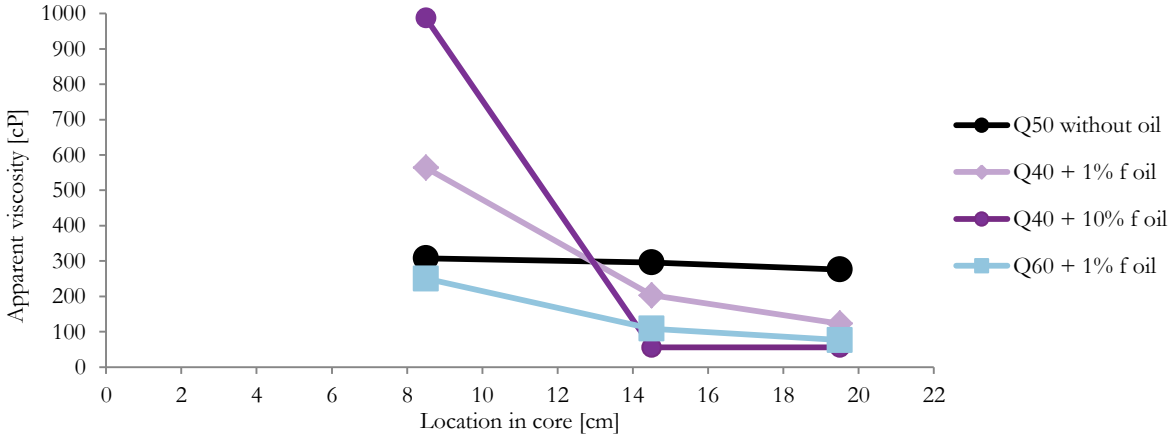

Figure 5.5: Apparent viscosity of pre-generated foam with surfactant A and oil over the length of the core. Q50: 50% foam quality, etc. f: fractional flow of oil in injected fluids.

5.4. Conclusions

We present a novel experimental approach to investigating the impact of oil on pre-generated foam at controlled oil flow rate. This approach allows one to investigate the weakening of pre-generated foam by oil as a function of distance travelled. Separate oil injection allows generation of foam without oil in the same porous medium before first contact with oil. The relatively narrow core diameter ensures rapid contact between foam and injected oil.

For the crude oil and surfactants examined here, pre-generated foam progressively weakened in presence of crude oil after first contact. The apparent viscosity in some cases decreased by more than a factor four over a distance of 0.15 m. We believe that in a sufficiently long core the pre-generated foam in contact with oil would gradually weaken until reaching the same apparent viscosity as with three-phase co-injection. Surprisingly, with surfactant A there is

an increase in apparent viscosity as foam first encounters the crude oil, before progressively weakening. We believe this reflects reduced gas and water relative permeabilities in three-phase flow, and possibly emulsification of oil in water.

Lower-quality foams propagated for a somewhat longer distance in the presence of oil than higher-quality foams, indicating that lower-quality foams are less susceptible (or less rapidly susceptible) to weakening by crude oil. (Distances in all cases are of course very short on a field scale.) Based on our experiments with 80% foam quality, we speculate that foam made with surfactant pre-equilibrated with the crude oil propagates for a shorter distance in presence of oil than foam made with surfactant that has not contacted oil before.

6. Conclusions and recommendations

In this dissertation, we developed insights on the flow behaviour of foam and crude oil in porous media. Moreover, we modelled the surfactant depletion at the gas-water interfaces in a porous media. Here we summarize the major conclusions of this work and give some recommendations for future research.

6.1. Effect of surfactant depletion by gas-water interfaces on foam stability in porous media

In chapter 2, we investigated the relation between surfactant depletion by the gas-water interface and the transition water-fraction (f_w^*), at which foam is at its minimum mobility in a porous medium. We proposed a simple model to estimate surfactant depletion at the gas-water interface at f_w^*. Furthermore, we analysed the effect of salt on surfactant depletion. We conclude the following:

- The fractions of surfactant depleted by the gas-water interface can be as much as 14% of the available surfactant in the injected liquid.
- For a given surfactant and salinity, surfactant depletion by the gas-water interface at f_w^* is roughly proportional to the surfactant concentration in the injectant.
- Increasing salinity results in decreasing f_w^*: foam can withstand drier conditions at higher salinity. Foams made with higher-salinity surfactant solutions, which increase the critical capillary pressure for foam-film stability and speeds the movement of surfactant molecules to the gas-water interface, can allow a greater depletion by the gas-water interface. Thus, in these cases a higher salinity results in a lower f_w^* at the same surfactant concentration. This suggests that an excess of surfactant to saturate the gas-water interface is required to achieve rapid saturation with surfactant of the gas-water interface. This mechanism is similar to the mechanism proposed by Jiménez and Radke (1989) for water transport to stretching film lamellae.

This work suggests an important connection between surfactant adsorption at gas-water interfaces and foam behaviour in porous media even far above the CMC. We recommend to further investigate the surfactant mass-transfer process in foam in porous media. Moreover, just like surfactant is depleted by the gas-water interfaces of foam in a porous medium, surfactant is depleted by the oil-water interfaces. We therefore recommend to investigate the depletion of surfactant by the oil-water interfaces and its impact on foam behaviour.

6.2. Impact of solubilized and dispersed oil on foam

In chapter 3 we investigated the impact of solubilized crude oil and hexane on foam in a porous medium and if it can explain the impact of crude oil and hexane on foam, as a separate phase. Moreover, we attempted to model the flow behaviour of a seawater solution (with and without surfactant), crude oil and nitrogen gas in a porous medium. We conclude the following:

- Experiments with solubilized crude-oil (pre-equilibrating our surfactant solution with crude oil or hexane) show that the impact of our solubilized crude oil on AOS foam is limited, and does not explain the behaviour we observe with three-phase co-injection. We do not observe significant impact of solubilized hexane on AOS foam in porous media, indicating that the large impact of dispersed hexane on AOS foam (Tang et al., 2018) cannot be accounted for by solubilized hexane.

- Experiments with crude oil co-injected with gas and water found that co-injection of crude oil, gas, and water (with and without surfactant) results in similar trends in apparent viscosity as a function of foam quality. With our simplified model, the apparent viscosities in three-phase-flow cannot be modelled with reduced gas mobility only; it requires reduced liquid (either water or oil) mobility as well. Furthermore, the apparent viscosity increases with increasing oil fractional flow (from 0.1% to 10%), which could be explained by the three-phase relative-permeability effects and emulsions generation in the core. Lastly, we did not observe foam in the effluent, though we did observe fast-collapsing foam when shaking a test-tube with crude oil and water (with and without surfactant).

We recommend to conduct core-flood experiments under a wider set of fractional flows to find if there is a relationship between the viscosity multiplier for the liquid phase (i.e., the effect of emulsions) and oil fractional flow. In the future, models should be explored that replicate the flow behaviour of water, oil, gas and some form of foam and emulsion.

6.3. Impact of crude oil on pre-generated foam

In Chapter 4 we presented a novel experimental approach to investigating the impact of oil on pre-generated foam with controlled oil flow rate. This approach allows one to investigate the weakening of pre-generated foam by oil as a function of distance travelled. Separate oil injection allows generation of foam without oil in the same porous medium before first contact with oil. The relatively narrow core diameter ensures rapid contact between foam and injected oil. We conclude the following:

- Pre-generated foam progressively weakened in presence of crude oil after first contact. The apparent viscosity can decrease by more than a factor four over a distance of 0.15 m. We speculate that in a sufficiently long core the pre-generated foam in contact with oil would gradually weaken until reaching the same apparent viscosity as with three-phase co-injection. Surprisingly, with surfactant A there is an increase in apparent viscosity as foam first encounters the crude oil, before progressively weakening. We believe this reflects reduced gas and water relative permeabilities in three-phase flow, and possibly emulsification of oil in water.
- Lower-quality foams propagated for a somewhat longer distance in the presence of oil than higher-quality foams, indicating that lower-quality foams are less susceptible (or less rapidly susceptible) to weakening by crude oil. (Distances in all cases are very short on a field scale.)
- In our case surfactant pre-equilibration with crude oil resulted in a foam more vulnerable to crude oil. Specifically our experiments with 80% foam quality suggest that foam made with surfactant pre-equilibrated with the crude oil propagates for a shorter distance in presence of oil than foam made with surfactant that has not contacted oil before.

We recommend to investigate the flow behaviour of in-situ pre-generated foam and different oils, and to compare that with the flow behaviour of co-injected surfactant, gas and oil, and with the impact of oil on pre-generated bulk foam and with the characteristics of bulk foam generated in presence of oil.

6.4. Impact of oil mixtures on foam

In chapter 5 we studied the effect of crude-oil composition on foam flooding. Crude oil is represented by a "synthetic" crude oil, composed of a mixture of several pure organic compounds (OC), with its composition based on the gas-chromatography analysis of the crude oil and its total acid number and total base number. The pure OCs represent the following chemical species in the crude oil: light and heavy alkanes, aromatics, cycloalkanes, organosulfur compounds, organic acid and organic base. The impact of the pure OCs and the "synthetic" crude oil on foam (in bulk and in porous media) is compared to the impact of the crude oil. We conclude the following:

- The effect of this crude oil on foam cannot be modelled by our synthetic crude oil. The impact of our synthetic crude oil is significantly less detrimental to foam than crude oil, both in bulk and in a porous medium. The impact of our synthetic crude oil is almost the same as our mixture of n-octane, hexadecane and oleic acid. This suggests that the other OCs added to our alkane mixture barely influenced the impact of our synthetic crude oil on foam, both in bulk and in a porous medium.
- Furthermore, it is not obvious how to correctly predict the impact of the OC mixture on a foam, based on a complete composition of an OC mixture. This holds even if the impact of all its components, separately, on foam are known. The impact of an OC mixture on foam is not necessarily the weighted average of the impact of the pure components, nor is its impact on foam necessarily skewed towards the impact of the most harmful component.
- In our case we find a good correlation between the foam apparent viscosity in a porous medium and the product of the bulk foam initial volume and half-life. This suggests that if either initial volume or half-life are poor for bulk foam the surfactant will perform poorly in the porous medium.

We recommend to verify if the correlation between the foam apparent viscosity and the product of the bulk foam half-life and initial volume holds for other OCs, foams and porous media. If this correlation holds in other cases as well, it can be used in the screening process of foam application for EOR. We suggest that, for now, crude-oil impact on foam should be tested with the crude oil itself. We could not correctly predict the impact of this crude oil on a specific foam based on the crude oil's composition determined from chromatography, TAN and TBN.

Although all the questions raised above are interesting, we recommend that a PhD candidate investigating the impact of (crude) oil on foam narrows his/her scope. Concerning the application of foam for EOR purposes, we recommend to account for the impact of emulsion generated on the flow behaviour of surfactant solution, oil and gas. This is because three-phase flow behaviour of foam and oil (without an emulsion) can be significantly different from the flow behaviour of foam and emulsion.

Appendix A

To model foam-free relative permeabilities in our three-phase co-injection experiments we use the experimental data of Alizadeh and Piri (2014). They conducted three-phase co-injection experiments in Bentheimer sandstone with a model oil (Soltrol 170), nitrogen and water without surfactant, and thus did not generate a foam or emulsion as in our experiments. They determined phase saturations using dual-energy computed tomography.

Figure A1 (a, b and c) show the relative-permeability data as a function of the phase saturations from Alizadeh and Piri (2014), and our modified Corey-model fits using to the parameters in Table 4.5. Alizadeh and Piri observe two gas relative-permeability relationships (Figure A1-c), one for increasing gas saturation and one for decreasing gas saturation, where there is some trapped gas in the porous medium. Because in our experiments we have foam in our porous medium, and thus trapped gas, we use the trend of decreasing gas saturation. Though the experiments of Alizadeh and Piri were also conducted with Bentheimer sandstone, our relative-permeability relationships might differ due to a different interfacial-tension (and wettability) between our crude oil and Bentheimer sandstone.

To model our experiments we first calculate the relative-permeability ratios of the different phases from the fractional-flow values; see equations Eq. A1 and Eq. A2. We then infer the phase saturations from the relative-permeability functions of the three phases, $k_{r,\alpha}$. We then calculate the three-phase mobilities and apparent viscosity using the relative-permeability values and viscosities of the phases, μ_α.

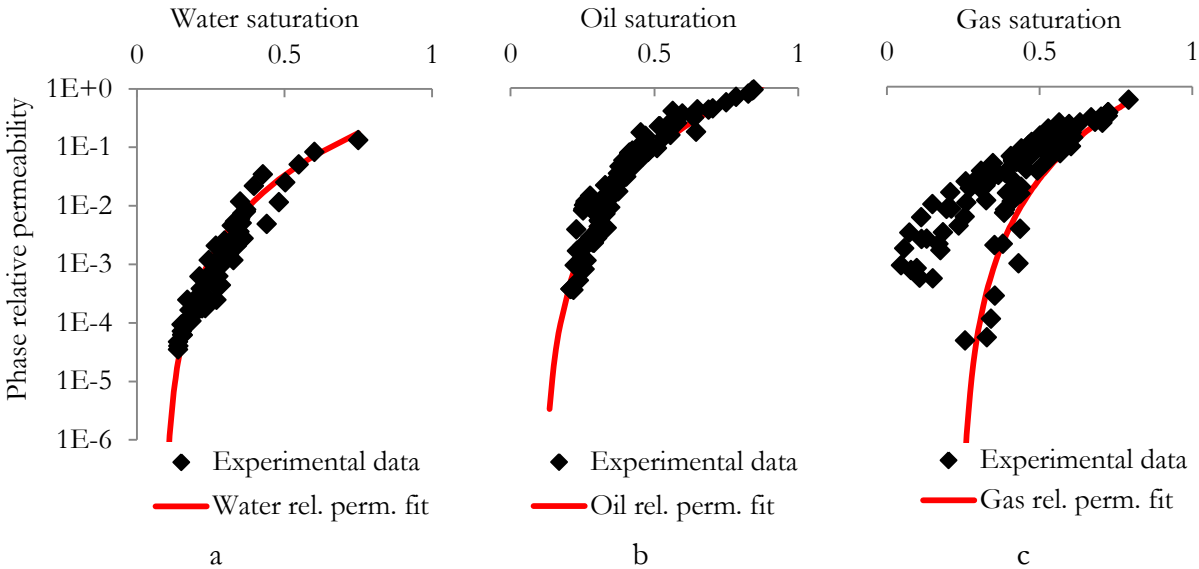

Figure A1: Three-phase relative-permeability experimental data, after Alizadeh and Piri (2014), and fit according to the parameters in Table 4.5. Note that we fit the gas relative-permeability trend from the data for decreasing gas saturation.

$$\frac{\frac{k_{r,\alpha}}{\mu_\alpha}}{\sum\frac{k_{r,i}}{\mu_i}} = f_\alpha$$ Eq. A1

$$\frac{f_\alpha \times \mu_\alpha}{\sum f_i \times \mu_i} = \frac{k_{r,\alpha}}{\sum k_{r,i}}$$ Eq. A2

Appendix B

Figure B1-a shows the model fit for the co-injection of water (without surfactant), gas, and crude oil (1% fractional-flow) and Figure B1-b shows the model fit for the co-injection of surfactant, gas and oil (0.1% fractional-flow). These figures are shown to illustrate that the proposed model can capture our observed three-phase flow behaviour with different fractional flows, with and without surfactant.

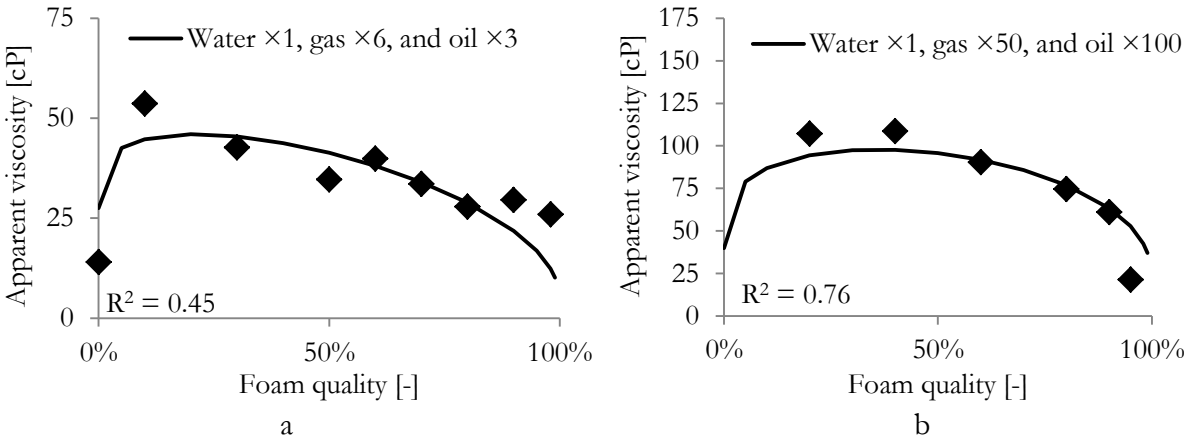

Figure B1: Apparent viscosities at different foam qualities in the three-phase co-injection experiments and their model fits. Figure a shows the experimental data obtained without surfactant in the aqueous phase, and 1% crude oil fractional flow, and the model fit with increased oil (×3) and gas viscosities (×6). Figure b shows the experimental data obtained with surfactant in the aqueous phase, and 0.1% crude oil fractional flow, and the model fit with increased oil (×100) and gas viscosities (×50).

Bibliography

Aarra, M.G., Skauge, A., 1994. A Foam Pilot in a North Sea Oil Reservoir: Preparation for a Production Well Treatment. Presented at the SPE Annual Technical Conference and Exhibition, Society of Petroleum Engineers. https://doi.org/10.2118/28599-MS

Alizadeh, A.H., Piri, M., 2014. The effect of saturation history on three-phase relative permeability: An experimental study. Water Resour. Res. 50, 1636–1664. https://doi.org/10.1002/2013WR014914

Alvarez, J.M., Rivas, H.J., Rossen, W.R., 2001. Unified Model for Steady-State Foam Behavior at High and Low Foam Qualities. SPE J. 6, 325–333. https://doi.org/10.2118/74141-PA

Andrianov, A., Farajzadeh, R., Mahmoodi Nick, M., Talanana, M., Zitha, P.L.J., 2012. Immiscible Foam for Enhancing Oil Recovery: Bulk and Porous Media Experiments. Ind. Eng. Chem. Res. 51, 2214–2226. https://doi.org/10.1021/ie201872v

Antón, R.E., Andérez, J.M., Bracho, C., Vejar, F., Salager, J.-L., 2008. Practical Surfactant Mixing Rules Based on the Attainment of Microemulsion–Oil–Water Three-Phase Behavior Systems, in: Narayanan, R. (Ed.), Interfacial Processes and Molecular Aggregation of Surfactants, Advances in Polymer Science. Springer Berlin Heidelberg, Berlin, Heidelberg, pp. 83–113.

Apaydin, O.G., Kovscek, A.R., 2001. Surfactant Concentration and End Effects on Foam Flow in Porous Media. Transp. Porous Media 43, 511–536. https://doi.org/10.1023/A:1010740811277

Arnaudov, L., Denkov, N.D., Surcheva, I., Durbut, P., Broze, G., Mehreteab, A., 2001. Effect of Oily Additives on Foamability and Foam Stability. 1. Role of Interfacial Properties. Langmuir 17, 6999–7010. https://doi.org/10.1021/la010600r

Bergeron, V., 1997. Disjoining Pressures and Film Stability of Alkyltrimethylammonium Bromide Foam Films. Langmuir 13, 3474–3482. https://doi.org/10.1021/la970004q

Bergeron, V., Fagan, M.E., Radke, C.J., 1993. Generalized entering coefficients: a criterion for foam stability against oil in porous media. Langmuir 9, 1704–1713. https://doi.org/10.1021/la00031a017

Bertin, H.J., Quintard, M.Y., Castanier, L.M., 1998. Modeling Transient Foam Flow in Porous Media Using a Bubble Population Correlation. Presented at the SPE Annual Technical Conference and Exhibition, Society of Petroleum Engineers. https://doi.org/10.2118/49020-MS

Boeije, C.S., Bennetzen, M.V., Rossen, W.R., 2017. A Methodology for Screening Surfactants for Foam Enhanced Oil Recovery in an Oil-Wet Reservoir. SPE Reserv. Eval. Eng. 20, 795–808. https://doi.org/10.2118/185182-PA

Boeije, C.S., Rossen, W., 2015. Fitting Foam-Simulation-Model Parameters to Data: I. Coinjection of Gas and Liquid. SPE Reserv. Eval. Eng. 18, 264–272. https://doi.org/10.2118/174544-PA

Bond, Holbrook, 1958. Gas drive oil recovery process. US2866507A.

Boos, J., Drenckhan, W., Stubenrauch, C., 2012. On How Surfactant Depletion during Foam Generation Influences Foam Properties. Langmuir 28, 9303–9310. https://doi.org/10.1021/la301140z

Chumpitaz, L.D.A., Coutinho, L.F., Meirelles, A.J.A., 1999. Surface tension of fatty acids and triglycerides. J. Am. Oil Chem. Soc. 76, 379–382. https://doi.org/10.1007/s11746-999-0245-6

Dalland, M., Hanssen, J.E., Kristiansen, T.S., 1994. Oil interaction with foams under static and flowing conditions in porous media. Colloids Surf. Physicochem. Eng. Asp. 82, 129–140. https://doi.org/10.1016/0927-7757(93)02628-R

Denkov, N.D., Marinova, K.G., Tcholakova, S.S., 2014. Mechanistic understanding of the modes of action of foam control agents. Adv. Colloid Interface Sci., Manuel G. Velarde 206, 57–67. https://doi.org/10.1016/j.cis.2013.08.004

Drenckhan, W., Saint-Jalmes, A., 2015. The science of foaming. Adv. Colloid Interface Sci., Reinhard Miller, Honorary Issue 222, 228–259. https://doi.org/10.1016/j.cis.2015.04.001
Eftekhari, A.A., Farajzadeh, R., 2017. Effect of Foam on Liquid Phase Mobility in Porous Media. Sci. Rep. 7, 43870. https://doi.org/10.1038/srep43870
Ettinger, R.A., Radke, C.J., 1992. Influence of Texture on Steady Foam Flow in Berea Sandstone. SPE Reserv. Eng. 7, 83–90. https://doi.org/10.2118/19688-PA
Fainerman, V.B., Lylyk, S.V., Aksenenko, E.V., Kovalchuk, N.M., Kovalchuk, V.I., Petkov, J.T., Miller, R., 2012. Effect of water hardness on surface tension and dilational visco-elasticity of sodium dodecyl sulphate solutions. J. Colloid Interface Sci. 377, 1–6. https://doi.org/10.1016/j.jcis.2012.03.030
Falls, A.H., Musters, J.J., Ratulowski, J., 1989. The Apparent Viscosity of Foams in Homogeneous Bead Packs. SPE Reserv. Eng. 4, 155–164. https://doi.org/10.2118/16048-PA
Farajzadeh, R., Andrianov, A., Krastev, R., Hirasaki, G.J., Rossen, W.R., 2012. Foam-oil interaction in porous media: implications for foam assisted enhanced oil recovery. Adv. Colloid Interface Sci. 183-184, 1–13. https://doi.org/10.1016/j.cis.2012.07.002
Gido, S.P., Hirt, D.E., Montgomery, S.M., Prud'homme, R.K., Rebenfeld, L., 1989. Foam Bubble Size Measured Using Image Analysis Before and After Passage Through a Porous Medium. J. Dispers. Sci. Technol. 10, 785–793. https://doi.org/10.1080/01932698908943199
Haynes, 2016. CRC Handbook of Chemistry and Physics, 97th ed.
Holm, L.W., Garrison, W.H., 1988. CO2 Diversion With Foam in an Immiscible CO2 Field Project. SPE Reserv. Eng. 3, 112–118. https://doi.org/10.2118/14963-PA
Jensen, J.A., Friedmann, F., 1987. Physical and Chemical Effects of an Oil Phase on the Propagation of Foam in Porous Media. Society of Petroleum Engineers. https://doi.org/10.2118/16375-MS
Jiménez, A.I., Radke, C.J., 1989. Dynamic Stability of Foam Lamellae Flowing Through a Periodically Constricted Pore, in: Oil-Field Chemistry, ACS Symposium Series. American Chemical Society, pp. 460–479.
Jones, S.A., Laskaris, G., Vincent-Bonnieu, S., Farajzadeh, R., Rossen, W.R., 2016a. Effect of surfactant concentration on foam: From coreflood experiments to implicit-texture foam-model parameters. J. Ind. Eng. Chem. 37, 268–276. https://doi.org/10.1016/j.jiec.2016.03.041
Jones, S.A., van der Bent, V., Farajzadeh, R., Rossen, W.R., Vincent-Bonnieu, S., 2016b. Surfactant screening for foam EOR: Correlation between bulk and core-flood experiments. Colloids Surf. Physicochem. Eng. Asp. 500, 166–176. https://doi.org/10.1016/j.colsurfa.2016.03.072
Kahrobaei, S., Farajzadeh, R., 2019. Insights into Effects of Surfactant Concentration on Foam Behavior in Porous Media. Energy Fuels. https://doi.org/10.1021/acs.energyfuels.8b03576
Kam, S.I., Rossen, W.R., 2003. A Model for Foam Generation in Homogeneous Media. SPE J. 8, 417–425. https://doi.org/10.2118/87334-PA
Kapetas, L., Vincent Bonnieu, S., Danelis, S., Rossen, W.R., Farajzadeh, R., Eftekhari, A.A., Mohd Shafian, S.R., Kamarul Bahrim, R.Z., 2015a. Effect of Temperature on Foam Flow in Porous Media. Society of Petroleum Engineers. https://doi.org/10.2118/172781-MS
Kapetas, L., Vincent-Bonnieu, S., Farajzadeh, R., Eftekhari, A.A., Mohd-Shafian, S.R., Bahrim, R.Z.K., Rossen, W.R., 2015b. Effect of Permeability on Foam-model parameters - An Integrated Approach from Coreflood Experiments through to Foam Diversion Calculations. Presented at the IOR 2015 - 18th European Symposium on Improved Oil Recovery. https://doi.org/10.3997/2214-4609.201412124

Khatib, Z.I., Hirasaki, G.J., Falls, A.H., 1988. Effects of Capillary Pressure on Coalescence and Phase Mobilities in Foams Flowing Through Porous Media. SPE Reserv. Eng. 3, 919–926. https://doi.org/10.2118/15442-PA

Khristov, K.I., Exerowa, D.R., Krugljakov, P.M., 1983. Influence of the type of foam films and the type of surfactant on foam stability. Colloid Polym. Sci. 261, 265–270. https://doi.org/10.1007/BF01469674

Kirk-Othmer, 2004. Encyclopedia of Chemical Technology, 5th ed.

Koczo, K., Lobo, L.A., Wasan, D.T., 1992. Effect of oil on foam stability: Aqueous foams stabilized by emulsions. J. Colloid Interface Sci. 150, 492–506. https://doi.org/10.1016/0021-9797(92)90218-B

Kornev, K.G., Neimark, A.V., Rozhkov, A.N., 1999. Foam in porous media: thermodynamic and hydrodynamic peculiarities. Adv. Colloid Interface Sci. 82, 127–187. https://doi.org/10.1016/S0001-8686(99)00013-5

Kristiansen, T.S., Holt, T., 1992. Properties of Flowing Foam in Porous Media Containing Oil. Presented at the SPE/DOE Enhanced Oil Recovery Symposium, Society of Petroleum Engineers. https://doi.org/10.2118/24182-MS

Lake, Johns, Rossen, Pope, 2014. Fundamentals of Enhanced Oil Recovery. Society of Petroleum Engineers, Richardson, Texas.

Langevin, 1992. Micelles and Microemulsions | Annual Review of Physical Chemistry.

Laskaris, 2015. Effect of Surfactant Concentration, Water Treatment Chemicals, Fatty Acids and Alcohols on Foam Behavior in Porous Media and in Bulk.

Lau, H.C., O'Brien, S.M., 1988. Effects of Spreading and Nonspreading Oils on Foam Propagation Through Porous Media. SPE Reserv. Eng. 3, 893–896. https://doi.org/10.2118/15668-PA

Lawson, J.B., Reisberg, J., 1980. Alternate Slugs Of Gas And Dilute Surfactant For Mobility Control During Chemical Flooding. Presented at the SPE/DOE Enhanced Oil Recovery Symposium, Society of Petroleum Engineers. https://doi.org/10.2118/8839-MS

Lee, H.O., Heller, J.P., 1990. Laboratory Measurements of CO2-Foam Mobility. SPE Reserv. Eng. 5, 193–197. https://doi.org/10.2118/17363-PA

Lee, J., Nikolov, A., Wasan, D., 2014. Effects of Micellar Structuring and Solubilized Oil on the Kinetic Stability of Aqueous Foams. Ind. Eng. Chem. Res. 53, 18891–18899. https://doi.org/10.1021/ie5014663

Lee, J., Nikolov, A., Wasan, D., 2013. Stability of Aqueous Foams in the Presence of Oil: On the Importance of Dispersed vs Solubilized Oil. Ind. Eng. Chem. Res. 52, 66–72. https://doi.org/10.1021/ie301102m

Lee, S., Kam, S.I., 2013. Chapter 2 - Enhanced Oil Recovery by Using CO2 Foams: Fundamentals and Field Applications, in: Sheng, J.J. (Ed.), Enhanced Oil Recovery Field Case Studies. Gulf Professional Publishing, Boston, pp. 23–61.

Lide, 2015. CRC Handbook of Chemistry & Physics, 96th ed.

Li, Y., Puerto, M., Bao, X., Zhang, W., Jin, J., Su, Z., Shen, S., Hirasaki, G., Miller, C., 2017. Synergism and Performance for Systems Containing Binary Mixtures of Anionic/Cationic Surfactants for Enhanced Oil Recovery. J. Surfactants Deterg. 20, 21–34. https://doi.org/10.1007/s11743-016-1892-x

Lobo, L.A., Nikolov, A.D., Wasan, D.T., 1989. Foam Stability in the Presence of Oil: On the Importance of the Second Virial Coefficient. J. Dispers. Sci. Technol. 10, 143–161. https://doi.org/10.1080/01932698908943167

Malvern Instruments, 2004. Zetasizer Nano Series User Manual, MAN0317. Malvern Instruments, Worcestershire, UK.

Manev, E., Scheludko, A., Exerowa, D., 1974. Effect of surfactant concentration on the critical thicknesses of liquid films. Colloid Polym. Sci. 252, 586–593. https://doi.org/10.1007/BF01558157

Manlowe, D.J., Radke, C.J., 1990. A Pore-Level Investigation of Foam/Oil Interactions in Porous Media. SPE Reserv. Eng. 5, 495–502. https://doi.org/10.2118/18069-PA
Mannhardt, K., Novosad, J.J., Schramm, L.L., 2000. Comparative Evaluation of Foam Stability to Oil. SPE Reserv. Eval. Eng. 3, 23–34. https://doi.org/10.2118/60686-PA
Mannhardt, K., Novosad, J.J., Schramm, L.L., 1998. Foam/Oil Interations at Reservoir Conditions. Society of Petroleum Engineers. https://doi.org/10.2118/39681-MS
Mannhardt, K., Svorstøl, I., 1999. Effect of oil saturation on foam propagation in Snorre reservoir core. J. Pet. Sci. Eng. 23, 189–200. https://doi.org/10.1016/S0920-4105(99)00016-9
Martin, F.D., Stevens, J.E., Harpole, K.J., 1995. CO_2-Foam Field Test at the East Vacuum Grayburg/San Andres Unit. SPE Reserv. Eng. 10, 266–272. https://doi.org/10.2118/27786-PA
Mast, R.F., 1972. Microscopic Behavior of Foam in Porous Media. Presented at the Fall Meeting of the Society of Petroleum Engineers of AIME, Society of Petroleum Engineers. https://doi.org/10.2118/3997-MS
Meling, T., Hanssen, J.E., 1990. Gas-blocking foams in porous media: effects of oil and surfactant hydrophobe carbon number, in: Lindman, B., Rosenholm, J.B., Stenius, P. (Eds.), Surfactants and Macromolecules: Self-Assembly at Interfaces and in Bulk, Progress in Colloid & Polymer Science. Steinkopff, pp. 140–154.
M.G. Aarra, A. Skauge, 2000. Status of foam applications in north sea reservoirs. Presented at the 21st Annual International Energy Agency Workshop and Symposium, Edinburgh.
Mitra-Kirtley, S., Mullins, O.C., Ralston, C.Y., Sellis, D., Pareis, C., 1998. Determination of Sulfur Species in Asphaltene, Resin, and Oil Fractions of Crude Oils. Appl. Spectrosc. 52, 1522–1525.
Moradi-Araghi, A., Johnston, E.L., Zornes, D.R., Harpole, K.J., 1997. Laboratory Evaluation of Surfactants for CO2-Foam Applications at the South Cowden Unit. Presented at the International Symposium on Oilfield Chemistry, Society of Petroleum Engineers. https://doi.org/10.2118/37218-MS
Mungan, N., 1965. Permeability Reduction Through Changes in pH and Salinity. J. Pet. Technol. 17, 1.449–1.453. https://doi.org/10.2118/1283-PA
Øren, P.-E., Bakke, S., 2003. Reconstruction of Berea sandstone and pore-scale modelling of wettability effects. J. Pet. Sci. Eng., Reservoir Wettability 39, 177–199. https://doi.org/10.1016/S0920-4105(03)00062-7
Osei-Bonsu, K., Grassia, P., Shokri, N., 2017. Investigation of foam flow in a 3D printed porous medium in the presence of oil. J. Colloid Interface Sci. 490, 850–858. https://doi.org/10.1016/j.jcis.2016.12.015
Patzek, T.W., 1996. Field Applications of Steam Foam for Mobility Improvement and Profile Control. SPE Reserv. Eng. 11, 79–86. https://doi.org/10.2118/29612-PA
Peksa, A.E., Wolf, K.-H.A.A., Zitha, P.L.J., 2015. Bentheimer sandstone revisited for experimental purposes. Mar. Pet. Geol. 67, 701–719. https://doi.org/10.1016/j.marpetgeo.2015.06.001
Pugh, R.J., 1996. Foaming, foam films, antifoaming and defoaming. Adv. Colloid Interface Sci. 64, 67–142. https://doi.org/10.1016/0001-8686(95)00280-4
Pu, W., Pang, S., Wang, C., 2017. Experimental investigation of foam performance in the presence of crude oil. J. Surfactants Deterg. 20, 1051–1059. https://doi.org/10.1007/s11743-017-1991-3
Raza, S.H., 1970. Foam in Porous Media: Characteristics and Potential Applications. Soc. Pet. Eng. J. 10, 328–336. https://doi.org/10.2118/2421-PA
Rosen, M.J., 2004. Surfactants and Interfacial Phenomena. John Wiley & Sons.

Rosen, M.J. with Hua, 1988. Dynamic surface tension of aqueous surfactant solutions: I. Basic paremeters. J. Colloid Interface Sci. 124, 652–659. https://doi.org/10.1016/0021-9797(88)90203-2

Rossen, W., Ocampo, A., Restrepo, A., Cifuentes, H., Marin, J., 2016. Long-Time Diversion in Surfactant-Alternating-Gas Foam Enhanced Oil Recovery From a Field Test. SPE Reserv. Eval. Eng. https://doi.org/10.2118/170809-PA

Schramm, L.L., Novosad, J.J., 1992. The destabilization of foams for improved oil recovery by crude oils: Effect of the nature of the oil. J. Pet. Sci. Eng., Enhanced Oil Recovery 7, 77–90. https://doi.org/10.1016/0920-4105(92)90010-X

Schramm, L.L., Novosad, J.J., 1990. Micro-visualization of foam interactions with a crude oil. Colloids Surf. 46, 21–43. https://doi.org/10.1016/0166-6622(90)80046-7

Schramm, L.L., Turta, A.T., Novosad, J.J., 1993. Microvisual and Coreflood Studies of Foam Interactions With a Light Crude Oil. SPE Reserv. Eng. 8, 201–206. https://doi.org/10.2118/20197-PA

Sharqawy, M.H., Lienhard, J.H., Zubair, S.M., 2010. Thermophysical properties of seawater: a review of existing correlations and data. Desalination Water Treat. 16, 354–380. https://doi.org/10.5004/dwt.2010.1079

Shi, S., Wang, Y., Bai, S., Li, Z., Ding, M., Chen, W., 2016. Pore-Scale Studies on the Stability of Microfoam and the Effect of Parameters on Its Bubble Size. J. Dispers. Sci. Technol. 37, 1019–1026. https://doi.org/10.1080/01932691.2015.1058168

Simjoo, M., 2012. Immiscible foam for enhanced oil recovery (PhD Dissertation). Delft University of Technology.

Simjoo, M., Rezaei, T., Andrianov, A., Zitha, P.L.J., 2013. Foam stability in the presence of oil: Effect of surfactant concentration and oil type. Colloids Surf. Physicochem. Eng. Asp. 438, 148–158. https://doi.org/10.1016/j.colsurfa.2013.05.062

Skauge, A., Aarra, M.G., Surguchev, L., Martinsen, H.A., Rasmussen, L., 2002. Foam-Assisted WAG: Experience from the Snorre Field. Society of Petroleum Engineers. https://doi.org/10.2118/75157-MS

Speight, J.G., 2014. The Chemistry and Technology of Petroleum, Fifth Edition. CRC Press.

Suffridge, R., 1989. Foam Performance Under Reservoir Conditions. https://doi.org/10.2118/19691-MS

Tang, 2019. The Effect of Oil on Foam for EOR (PhD Dissertation). Delft University of Technology.

Tang, G.-Q., Kovscek, A.R., 2006. Trapped Gas Fraction During Steady-State Foam Flow. Transp. Porous Media 65, 287–307. https://doi.org/10.1007/s11242-005-6093-4

Tang, J., Vincent-Bonnieu, S., Rossen, W., 2018a. Experimental Investigation of the Effect of Oil on Steady-State Foam Flow in Porous Media. SPE J. https://doi.org/10.2118/194015-PA

Tang, J., Vincent-Bonnieu, S., Rossen, W., 2018b. Experimental Investigation of the Effect of Oil on Steady-State Foam Flow in Porous Media. SPE J. https://doi.org/10.2118/194015-PA

Tcholakova, S., Denkov, N.D., Danner, T., 2004. Role of Surfactant Type and Concentration for the Mean Drop Size during Emulsification in Turbulent Flow. Langmuir 20, 7444–7458. https://doi.org/10.1021/la049335a

Tcholakova, S., Denkov, N.D., Sidzhakova, D., Ivanov, I.B., Campbell, B., 2003. Interrelation between Drop Size and Protein Adsorption at Various Emulsification Conditions. Langmuir 19, 5640–5649. https://doi.org/10.1021/la034411f

Texas Administrative Code, n.d. Texas Statewide Spacing Rule 37 [WWW Document]. URL https://texreg.sos.state.tx.us/public/readtac$ext.TacPage?sl=R&app=9&p_dir=&p_rloc=&p_tloc=&p_ploc=&pg=1&p_tac=&ti=16&pt=1&ch=3&rl=37 (accessed 8.7.18).

Turta, A.T., Singhal, A.K., 2002. Field Foam Applications in Enhanced Oil Recovery Projects: Screening and Design Aspects. J. Can. Pet. Technol. 41. https://doi.org/10.2118/02-10-14

Tuvell, M.E., Kuehnhanss, G.O., Heidebrecht, G.D., Hu, P.C., Zielinski, A.D., 1978. AOS — An anionic surfactant system: Its manufacture, composition, properties, and potential application. J. Am. Oil Chem. Soc. 55, 70–80. https://doi.org/10.1007/BF02673393

Van der Bent, 2014. Comparative study of foam stability in bulk and porous media. Delft University of Technology.

Vikingstad, A.K., Skauge, A., Høiland, H., Aarra, M., 2005. Foam–oil interactions analyzed by static foam tests. Colloids Surf. Physicochem. Eng. Asp. 260, 189–198. https://doi.org/10.1016/j.colsurfa.2005.02.034

Zhang, H., Miller, C.A., Garrett, P.R., Raney, K.H., 2003. Mechanism for defoaming by oils and calcium soap in aqueous systems. J. Colloid Interface Sci. 263, 633–644. https://doi.org/10.1016/S0021-9797(03)00367-9

Nomenclature

A_b Surface area of a foam bubble with radius r_b [m^2]
A_s Surface area covered by a unit mass of surfactant [m^2/kg]
C_s Surfactant concentration of solution [wt.%]
$C_{s,b}$ Surfactant concentration in aqueous phase, including only surfactant in bulk of solution (not at interface) [wt.%]
$C_{s,i}$ Surfactant concentration in aqueous phase, including only surfactant on gas-water interface [wt.%]
f_g Gas fractional flow [-]
f_g^* Transition gas fractional flow [-]
f_o Oil fractional flow [-]
f_w Water fractional flow [-]
f_w^* Transition water fractional flow [-]
k Permeability [m^2]
$k_{r,\alpha}$ Relative permeability to phase α [-]
$k^o_{r,\alpha}$ End-point relative-permeability [-]
μ_{app} Apparent viscosity of foam [cP]
n_α Corey parameter [-]
P_c^* Limiting capillary pressure [Pa]
∇P Pressure gradient [bar/m]
q Total superficial velocity [m/s]
r_b Typical gas bubble radius [m]
ρ_s Surfactant solution density [kg/m^2]
S_α Saturation of phase α [-]
$S_{r,\alpha}$ Residual saturation of phase α [-]
V_b Volume of a foam bubble with radius r_b [m^3]
Z $C_{s,b}/C_{s,i}$ [-]

Summary

Foam flooding can be applied in soil-remediation techniques or for improving oil recovery processes in petroleum reservoirs. There are models which aim to predict the behaviour of foam in presence of oil in bulk and in porous media, however these models are not very reliable. In this work we investigate different ways in which a specific crude oil impacts a specific foam in a porous medium. Furthermore, we model surfactant depletion by the gas-water interface, which can partly explain the transition from the low-quality to the high-quality regime of foam in porous media.

Foam in porous media coarsens below a transition water fractional flow f_w^*. This transition corresponds to the onset of the "high-quality" regime in which foam is at its limit of stability. The relationship between surfactant concentrations above the critical micelle concentration (CMC) and f_w^* is not well understood. The surfactant effect on foam film stability is negligible above the CMC. In **Chapter 2** we investigate the relation between surfactant depletion by the gas-water interface and f_w^*. Our analysis of experimental data shows that, for a specific porous medium and surfactant, f_w^* decreases rapidly with the surfactant concentration at low concentrations and approaches a constant value at high concentrations. We find that the surfactant depletion by the gas-water interface at f_w^* is roughly proportional to the surfactant concentration in the injectant. This correlation relates f_w^* to surfactant concentration. We find that this proportionality is dependent on the solution salinity, in line with the previously findings for the salinity effect on the critical capillary pressure for foam films. By including an adjustable parameter for the different salinities, we can quantitatively match the experimental data.

Currently, to understand and model the behaviour of foam in an oil reservoir, experiments need to be conducted in the presence of the specific crude oil. A model which can forecast the impact of a crude oil on foam solely based on the crude oil composition would allow one to efficiently screen reservoirs for foam application. In **Chapter 3** we investigate the behaviour of foam in the presence of a crude oil, and in the presence of mixtures of pure components. We form a "synthetic" crude oil, with its composition mimicking the composition of a crude oil and the total acid/base number. Although the pure OC and synthetic crude oil weaken the foam in the bulk and in porous media, their impact on foam is less severe than the impact of the crude oil on the foam. Based on the composition of an oil mixture and the impact of its separate components on the foam, it is not obvious how to correctly predict the impact of the oil mixture on bulk foam or on foam in a porous medium. However, in our case we find a good correlation between the foam apparent viscosity in porous media and the product of the bulk foam half-life and initial volume. One implication is that if either the half-life or initial volume of bulk foam is poor, the foam performs poorly in the porous medium.

In **Chapter 4** we investigate whether the behaviour of steady-state foam with crude oil can be explained by solubilized oil components. We perform foam-flooding experiments with a surfactant solution previously equilibrated with crude oil. The impact of crude oil, as a separate, dispersed oleic phase, is studied here by co-injection of crude oil, surfactant solution and gas in core-floods, focusing on steady-state mobility, captured by the pressure gradient within the core. In this case crude oil, as a separate oleic phase, reduces the pressure gradient within the core up to a factor of twenty compared to the case without oil. Nonetheless, this pressure gradient is about a factor three larger than what we observe by co-injecting crude oil, water without surfactant, and gas. With a simplified model we fit our three-phase co-injection experimental data

by increasing the viscosity of both the gas and water, indicating that some weak foam and emulsion is generated. Neither effect by itself can fit the data. In contrast, with crude oil solubilized in the surfactant solution, the pressure gradient is of the same order of magnitude as for co-injection gas and surfactant with or without solubilized oil. These results indicate that solubilized crude oil does not reduce the foam mobility as much as does the crude oil as a separate oleic phase. Furthermore, the effect of solubilized crude on foam is not due only to straight-chain aliphatic components such as hexane: our experiment with solubilized hexane showed a less-significant impact on foam mobility.

Furthermore, we investigate the behaviour of foam in presence of crude oil in porous media. In **Chapter 5** we present a novel experimental method to investigate the impact of oil on in-situ pre-generated foam in a porous medium. This approach allows us to generate foam in the absence of oil and then to examine the effect of subsequent oil contact, in a single porous medium. Our experimental results indicate that foam and crude oil reach steady-state almost instantaneously compared to the length of a reservoir-simulation grid-block. This study extends previous micro-model studies on the impact of oil on in-situ generated foam to conditions that look more like those in actual field applications. Dispersed and solubilized oil can impact the bulk foam stability differently. Although aromatic components are more soluble in water than straight-chain aliphatic components, solubilized aromatics do not necessarily impact the stability of foam in bulk or porous media, whereas straight-chain aliphatic components can have a detrimental impact (Bergeron et al., 1993; Lee et al., 2013). However, to our knowledge there is no published research on the impact of a solubilized crude oil on foam, as distinct from a separate oil phase, in a porous medium.

Samenvatting

Schuimstroming kan onder meer worden toegepast als een methode voor het saneren van verontreinigde grond of als een manier om meer olie uit een reservoir te verkrijgen (Engels: Enhanced Oil Recovery (EOR)). Er bestaan modellen voor het voorspellen van het gedrag van schuim in een poreus medium in de aanwezigheid van olie. Deze modellen zijn echter niet erg betrouwbaar. In dit proefschrift onderzoeken wij verschillende manieren waarop een specifieke aardolie invloed heeft op het schuim in een poreus medium. Daarnaast modelleren wij de adsorptie van oppervlakte-actieve stoffen (Engels: surfactants) op het gas-water grensoppervlak van de schuimbellen in een poreus medium. Dit kan gedeeltelijk een verklaring geven voor de overgang van het zogenaamde *lage kwaliteit* schuimregime naar het *hoge kwaliteit* schuimregime in een poreus medium.

Schuim in een poreus medium wordt grover beneden een bepaalde overgangswaarde van de waterfractie van het debiet**,** f_w^*. Deze overgangswaarde van de waterfractie van het debiet komt overeen met de aanvang van de *hoge kwaliteit* schuimregime, waar het schuim de grens van zijn stabiliteit heeft bereikt. De relatie tussen f_w^* en de surfactant concentratie, boven de kritische waarde van de micelconcentratie (Engels: critical micelle concentration (CMC)), is niet goed begrepen. Dit komt onder meer doordat de invloed van de surfactant concentratie op de stabiliteit van zeepfilms verwaarloosbaar is boven de CMC. In **hoofdstuk 2** onderzoeken wij de relatie tussen f_w^* en de surfactant uitputting door het gas-water grensoppervlak. Onze analyse van experimentele data toont aan dat, voor een specifiek poreus medium met schuim, f_w^* sterk daalt met de surfactant concentratie bij een lage surfactant concentratie, terwijl f_w^* een constante waarde nadert bij een hoge surfactant concentratie. Onze bevinding is dat de surfactant uitputting door het gas-water oppervlak bij f_w^* grofweg proportioneel is met de surfactant concentratie in de geïnjecteerde vloeistof. Deze bevinding correleert f_w^* aan de surfactant concentratie. Daarnaast vinden wij dat de proportionaliteit afhankelijk is van de zoutconcentratie in de surfactant oplossing. Dit is in overeenstemming met eerdere bevindingen over de invloed van de zoutconcentratie in de surfactant oplossing op de kritische capillaire druk van zeepfilms. Door een variabele toe te voegen voor de verschillende zoutconcentraties kunnen wij de experimentele data kwalitatief reproduceren.

Bij de huidige manier om de invloed van aardolie op zeepschuim in een olieveld te begrijpen en te modeleren moeten er eerst experimenten uitgevoerd worden met de specifieke aardolie. Een model waarmee de invloed van een aardolie op schuim kan worden voorspeld op basis van de samenstelling van de aardolie zou men kunnen gebruiken om op een efficiënte wijze olievelden te evalueren voor het toepassen van schuimstroming voor EOR. In **Hoofdstuk 3** onderzoeken wij met behulp van doorstromingsexperimenten het gedrag van schuim in de aanwezigheid van aardolie en in de aanwezigheid van pure componenten, in de bulk en in een poreus. Daartoe maken wij een "synthetische" aardolie, met een samenstelling die overeenkomt met de samenstelling van de aardolie en diens waarden voor zuur en base. Het blijkt dat de pure organische componenten en de synthetische aardolie een verzwakkend effect hebben op het schuim, alhoewel in mindere mate dan voor aardolie. Wij concluderen dat er op basis van de samenstelling van een oliemengsel en de invloed van de afzonderlijke componenten op een schuim er geen voor de hand liggend methode is om de invloed van het oliemengsel op schuim te voorspellen. Desalniettemin vinden wij een goede correlatie tussen de schijnbare viscositeit van het schuim in een poreus medium en het product van het initiële volume en de halveringstijd van

het bulkschuim. Dit impliceert dat als een bulkschuim een korte halveringstijd of een klein initieel volume heeft, het schuim in een poreus medium zwak zal zijn.

In **hoofdstuk 4** onderzoeken wij of de stabiele toestand van schuim met aardolie verklaard kan worden vanuit de opgeloste olie componenten. Daartoe hebben wij doorstromingsexperimenten met schuim uitgevoerd via een surfactant oplossing dat in evenwicht is gebracht met aardolie. De invloed van aardolie, in de olie-fase, op schuim is hierbij onderzocht door aardolie, surfactant oplossing en gas samen te injecteren in een kern. Hierbij letten we vooral op de mobiliteit in stabiele toestand. De mobiliteit komt tot uitdrukking als de drukgradiënt over de kern. Wanneer wij aardolie, surfactant oplossing en gas samen injecteren, meten wij een drukgradiënt over de kern die tot een factor twintig lager is in vergelijking met wat gevonden wordt bij het tezamen injecteren van surfactant oplossing en gas, zonder olie. Echter, de drukgradiënt is ongeveer een factor drie hoger dan wat wij hebben gemeten bij het tezamen injecteren van aardolie, gas en water (zonder surfactant). Met een simpel model kunnen wij het geobserveerde gedrag bij de drie-fasen injectie experimenten nabootsen. In dit model moet de viscositeit van gas én water verhoogd worden om het geobserveerde gedrag te reproduceren, wat aangeeft dat er een (zwak) schuim en emulsie worden gevormd in de experimenten. Wij kunnen onze metingen niet nabootsen door alleen de gas viscositeit of alleen de water viscositeit te verhogen. Ter vergelijking, bij een doorstromingsexperiment met schuim, via onze surfactant oplossing dat opgeloste aardolie bevat, is de drukgradiënt over de kern ongeveer even hoog als bij ons doorstromingsexperiment met schuim via een surfactant oplossing zonder opgeloste aardolie. Deze bevindingen duiden aan dat de opgeloste olie de schuimmobiliteit minder verhoogt dan aardolie in de oliefase. Bovendien tonen wij aan dat het effect van onze opgeloste aardolie op schuim niet alleen wordt veroorzaakt door de acyclische alifatische componenten, zoals hexaan. Onze experimenten met opgelost hexaan geven een minder significante invloed op schuim dan opgeloste aardolie.

Wij hebben ook gekeken naar het gedrag van voor-gegenereerde schuim in de aanwezigheid van aardolie in een poreus medium. In **hoofdstuk 5** presenteren wij een nieuwe experimentele methode voor het onderzoeken van de invloed van aardolie op in-situ voor-gegenereerde schuim in een poreus medium. Deze methode maakt het mogelijk om schuim te genereren in de afwezigheid van olie en vervolgens de invloed van olie op het schuim te onderzoeken in één poreus medium. De meetresultaten laten zien dat met onze methode het schuim en de aardolie vrijwel direct een stabiele toestand bereiken. Dit onderzoek vormt een uitbreiding van eerdere micro-model studies naar de invloed van olie op in-situ gegenereerde schuim naar condities die meer lijken op de werkelijke veldomstandigheden.

Acknowledgements

I offer my sincerest gratitude to my thesis supervisors Prof. Bill Rossen and Dr. Sébastien Vincent-Bonnieu. Thank you for offering me this wonderful opportunity to develop myself as a scientist and as a person. Thank you both for supporting me throughout my PhD project with your patience and knowledge whilst allowing me to work in my own way. Although our weekly meetings only lasted (usually a bit more than) 45 minutes, each meeting contributed more than a full day work. Somehow, each week I was more energized by the time I stepped out of the meeting.

Thank you Bill for creating a warm atmosphere in the foam group by organizing a weekly lunch & coffee and having a weekly foam-group meeting. The yearly foam-group dinner was something I looked forward to. This created an atmosphere fit for collaboration. Your knowledge on foam and flow through porous media was astounding and crucial for the successful execution of this project. In the past four years I have learnt a lot from you on how to conduct, write and judge scientific research, and it will take me many more years to reach your level of expertise. It is truly inspiring. Thank you for allowing me to fulfil my curiosity cravings by spending time on a numerous courses, conferences and workshops, and various side-projects. I am convinced all these activities contributed to produce a better PhD dissertation. Thank you Janice for sharing your optimism and enthusiasm, whenever we meet (or when I think of your kind words) I feel like I can take on the world.

Sébastien, no matter how busy you were with your duties at Shell, you always made time to be present at the meetings, lunches, and yearly meetings,. You taught me how to be efficient in meetings; even when we had many topics to discuss in a meeting you made sure that we did not extend the meeting by too much time. You taught me how to be a good supervisor to my thesis students, and whenever I wasn't sure what to do as a supervisor I would recall how you supervised me as an MSc student. Thank you for connecting me with the relevant researchers and motivating me to go to the interesting conferences. Thanks to you I became part of the foam community, which contributed to my dissertation. You motivated me in my side-projects, this made me enjoy the work even more. As a supervisor you gave me the confidence to conduct my experiments in my own way and trust in my own expertise.

I wish to appreciate all the members of the Dietz lab that contributed through good advice and their good spirits to this thesis. Many thanks go to Michiel Slob for helping me to set up the experimental apparatus, without your help this research would have taken a much longer time to finish. I would also like to thank Ellen, Jolanda, Mark and Karel for your expertise in the lab.

A special thank you to the administrative side of the Geosciences and Engineering department, Marlijn, Lydia, Margot, Ralf, Marja and Marijke, for your compassionate support.

Prof. Hans Bruining, Prof. Denis Voskov and Prof. Karl-Heinz Wolf, thank you for sharing your expertise whenever I had any questions, this team spirit is what makes working at our department so wonderful.

In addition, I am grateful to my doctoral defence committee Prof. Henri Bertin, Prof. Julia Gebert, Prof. Ruud Henkes, Prof. Ismail Saaid, Prof. Pacelli Zitha for reviewing my dissertation and giving valuable comments.

I would like to thank Universiti Teknologi PETRONAS for sponsoring this research. The bi-annual meetings we had together with PETRONAS and Shell were a great source of useful

insights. Dr. Ivy Chai Ching Hsia and Ridhwan Bahrim of PETRONAS, you were always ready to help me with your technical knowledge, and without your help I would still be stuck trying to solve many puzzling questions. I would also like to thank Dr. Jeroen Groenenboom, Chris Parsons, Erik van der Weerd, Dr. Rashidah Pilus, Dr. Hans Groot, Prof. Mariyamni Awang.

I would like to thank Prof. Steven Abbot and Prof. Reinhard Miller for advice on surfactant depletion by the gas-water interface. Prof. Ger Koper, thank you for allowing me to conduct measurements on your Dynamic Light Scattering device and for sharing your knowledge with me.

To my thesis students: Aran Amin, Adhitomo Sulistyo, Mauricio Sotomayor and Minh Bui, I learnt a lot from you, be it your unique ways of analysing and solving problems, project management or your personal demeanours. You all did wonderfully in your projects and I am sure you would have done wonderfully without my involvement, it makes me proud that you voluntarily chose to involve me in your projects.

Sian, you were a source of joy, knowledge and sweets. Martijn and Swej I enjoyed working with you on the same project and had a lot of fun on our trips abroad. Bander, Guanqun, Jiakun, Kiarash, Kai, Xiaocong, Raphael, Nikita, Jinyu, Rodrigo, Mark, Matei, Matteo, Yang, Chris, Rahul Durgesh, Siavash, Mojtaba, Siamak, Amin, Mohsen Faisal, Baptiste, Eduardo, and all my other colleagues and friends at the university, working at TU Delft was a pleasure thanks to all of you.

Georgios, thank you for creating fun weekends with your vibrating energy and bottomless well of exciting stories. Romano, your persistence and optimism are an example to me. Nakul and Sujaya, thank you for the nice dinners and discussion, and a special thanks from our cat, Jopie, for hosting when Lara and I were travelling. Max, thank you for hosting in Stavanger, it was a wonderful weekend. Martijn and Ebin, our trip to India was amazing. Marcel, Guido, Jules, Praveen, Lara M., Audrey, Djamal, Omar, Abdul, Fabian and Maarten, thank you for all the dinners, lunches, and early coffees.

Words cannot express my gratitude to my lovely wife Lara. Your positivity and enthusiasm makes any situation more joyful. Thank you for listening to my stories every day. Thank you for bringing our cat, Jopie, into our lives. Thank you for supporting me in my cooking and baking adventures. Thank you for supporting me during my PhD with your positive mentality. Thank you for being there whenever I need you. Thank you Lara.

I would like to express my deepest thanks to my family and family-in-law. I am extremely thankful to my parents for their love and blessings, and for their patience in these years. I am grateful to my brothers and my sister-in-law for your support. Dahlia, my lovely niece, although you are only two years old, your energy and strong character are admirable.

Ahmed Hussain,
June 2019

Scientific contributions

Journal articles

- Hussain, A. A. A., Vincent-Bonnieu, S., Kamarul Bahrim, R.Z., Pilus, R. M. and Rossen, W.R., 2019, Impact of different oil mixtures on foam in porous media and in bulk. *Journal of Industrial and Engineering Chemistry Research*

- Hussain, A. A. A., Vincent-Bonnieu, S., Kamarul Bahrim, R.Z., and Rossen, W.R. The impacts of solubilized and dispersed crude oil on foam in a porous medium. *Submitted to a journal*

- Hussain, A. A. A., Vincent-Bonnieu, S., Pilus, R. M. and Rossen, W.R. Effect of surfactant depletion by gas water interfaces on foam stability in porous media. *Submitted to a journal*

- Hussain, A. A. A., Vincent-Bonnieu, S., Kamarul Bahrim, R.Z., Pilus, R. M. and Rossen, W.R., Impact of crude oil on pre-generated foam in porous media. *Submitted to a journal*

Conference proceedings and talks

- Hussain, A. A. A., Vincent-Bonnieu, S., Kamarul Bahrim, R.Z., Pilus, R. M. and Rossen, W.R., Impact of crude oil on pre-generated foam in porous media. Presented at the *20th European Symposium on Improved Oil Recovery*, (We A 07), Pau, France, 8-10 April 2019, https://doi.org/10.3997/2214-4609.201900146

- Hussain, A. A. A., Vincent-Bonnieu, S., Kamarul Bahrim, R. M. and Rossen, W.R., Impact of solubilized and dispersed crude oil on foam in a porous medium, Presented at the *12th EUFOAM conference*, Liège, Belgium, 10 – 12 July, 2018

- Hussain, A. A. A., Vincent-Bonnieu and Rossen, W.R., Impact of surfactant depletion on foam in porous media, Presented at the *16th Conference of the International Association of Colloid and Interface Scientists*, Rotterdam, The Netherlands, 21 – 25 May 2018

- Hussain, A. A. A., Vincent-Bonnieu and Rossen, W.R., Impact of surfactant depletion on foam in porous media, Poster presented at the *7th Bubble & Drop conference*, Lyon, France, 26 – 30 June 2017

- Hussain, A.A.A., Amin, A., Vincent-Bonnieu, S., Farajzadeh, R., Andrianov, A., Abdul Hamid, P. and Rossen W.R., Effect of oil on gravity segregation in SAG foam flooding. Poster presented at the *19th European Symposium on Improved Oil Recovery*, (We P005), Stavanger, Norway, 24-27 April 2017, https://doi.org/10.3997/2214-4609.201700342

- Hussain, A.A.A., Amin, A., Vincent-Bonnieu, S., Farajzadeh, R., Andrianov, A., Abdul Hamid, P. and Rossen W.R., Foam Front Propagation Through a Water-Flooded Oil Reservoir, (#1570258118)*,* Presented at the *Fourth International Conference on Integrated Petroleum Engineering and Geosciences,* Kuala Lumpur, Malaysia, 15-17 August 2016

About the author

Ahmed Hussain was born on February 20th, 1990, in Zaanstad, The Netherlands. In 2013 he obtained his MSc degree from Delft University of Technology in Applied Earth Sciences, specialising in Petroleum Engineering. During his time at the university he completed three internships (two in oil & gas and one in finance) and was a board-member of the local SPE student chapter. From 2013 to 2015 he worked as a Reservoir Engineer at Tulip Oil. In July 2015 he started his PhD project at Delft University of Technology under the supervision of Prof. dr. Bill Rossen and Dr. Sébastien Vincent-Bonnieu.

Besides conducting research, the author enjoys cooking, sporting and travelling. He competed in the Dutch version of the Great British Bake Off (Heel Holland Bakt) and competed in the Dutch student boxing-championship. He has travelled to all continents, except for Antarctica.